T.C.

ÇANAKKALE ONSEKIZ MART UNIVERSITY

SCHOOL OF GRADUATE STUDIES

DEPARTMENT OF MOLECULAR BIOLOGY AND GENETIC

MOLECULAR AND BIOINFORMATIC IDENTIFICATION OF TWO STEROL METHYLTRANSFERASES WHICH ARE INVOLVED IN PLANT STEROL BIOSYNTHESIS IN OLIVE (*Olea europaea* L.)

MASTER OF SCIENCE THESIS

KÜBRA ÖZTÜRK

Thesis Supervisor

PROF. DR. KEMAL MELİH TAŞKIN

ÇANAKKALE – 2023

T.C.

ÇANAKKALE ONSEKIZ MART UNIVERSITY

SCHOOL OF GRADUATE STUDIES

DEPARTMENT OF MOLECULAR BIOLOGY AND GENETIC

MOLECULAR AND BIOINFORMATIC IDENTIFICATION OF TWO STEROL METHYLTRANSFERASES WHICH ARE INVOLVED IN PLANT STEROL BIOSYNTHESIS IN OLIVE (*Olea europaea L.)*

MASTER OF SCIENCE THESIS

KÜBRA ÖZTÜRK

Thesis Supervisor

PROF. DR. KEMAL MELİH TAŞKIN

This study has been supported by The Scientific and Technological Research Council of Türkiye

Project No: 118O405

ÇANAKKALE – 2023

ETİK BEYAN/ PLAGIARISM DECLARATION

Çanakkale Onsekiz Mart Üniversitesi Lisansüstü Eğitim Enstitüsü Tez Yazım Kuralları'na uygun olarak hazırladığım bu tez çalışmasında; tez içinde sunduğum verileri, bilgileri ve dokümanları akademik ve etik kurallar çerçevesinde elde ettiğimi, tüm bilgi, belge, değerlendirme ve sonuçları bilimsel etik ve ahlak kurallarına uygun olarak sunduğumu, tez çalışmasında yararlandığım eserlerin tümüne uygun atıfta bulunarak kaynak gösterdiğimi, kullanılan verilerde herhangi bir değişiklik yapmadığımı, bu tezde sunduğum çalışmanın özgün olduğunu, bildirir, aksi bir durumda aleyhime doğabilecek tüm hak kayıplarını kabullendiğimi taahhüt ve beyan ederim.

I declare that all the information and results offered in visual, audio, and written form are obtained by myself observing the academic and ethical rules. Moreover, all other results and information referred in the thesis but not specific to this study are cited.

Kübra ÖZTÜRK

30/01/2023

ACKNOWLEDGEMENTS

I would like to present my admiration and genuine gratitude to my esteemed supervisor, Prof. Dr. Kemal Melih TAŞKIN, for his unwavering support and guidance throughout the writing process of this thesis. I also would like to thank him deeply for giving me the chance to improve myself as a qualified scientist with his patience, effort, and kindness.

Especially, I would like to express my sincere gratitude to Dr. Fatih SEZER and Dr. Aslıhan ÖZBİLEN, for teaching me everything and helping me overcome any difficulty. Their guidance always lighted my way and gave me courage.

I would like to extend my sincere gratitude to the thesis committee and members of juries for their attention and time.

I would like to express my endless love and thanks to my dear friends, Cansu KARAKURT, Buket ÜNER, and Göktuğ SERBEZLER, who made me feel a sense of solidarity, trust, friendship, and teamwork. I would also like to thank the KMTLAB team Ali, İrem, Ezgi, and Hasan, who did not spare me their help in my studies.

My eternal gratitude goes to my beloved mother Ayşe ÖZTÜRK and my dad Canip ÖZTÜRK for supporting and believing me in all my education life. I am also eternally grateful to my sisters Tuba ÖZTÜRK and Esma ÖZTÜRK and my brother Mehmet ÖZTÜRK for supporting me every moment of my life.

Lastly, I would like to extend my heartfelt thanks M. Mert ÇELİKAY for never giving up to believe in me and encourage me to make happen my dreams.

For their financial support, I would like to thank The Scientific and Technological Research Council of Turkey (Project No: 118O405).

Kübra ÖZTÜRK

Çanakkale, January 2023

ÖZET

BİTKİ STEROL BİYOSENTEZİNDE GÖREV ALAN İKİ STEROL METİLTRANSFERAZ GENİNİN MOLEKÜLER VE BİYOİNFORMATİK OLARAK ZEYTİN (*Olea europaea* L.) GENOMUNDA TANIMLANMASI

Kübra ÖZTÜRK
Çanakkale Onsekiz Mart Üniversitesi
Lisansüstü Eğitim Enstitüsü
Moleküler Biyoloji ve Genetik Anabilim Dalı Yüksek Lisans Tezi
Danışman: Prof. Dr. Kemal Melih TAŞKIN
30.01.2023, 59

Fitosteroller (PSs) olarak bilinen bitki fotokimyasalları son dönemlerde insan sağlığına olan çeşitli faydalarından dolayı bilimsel camiada birçok çalışmanın odağı haline gelmiştir. Bitkilerde hücre zarının temel yapıtaşı olan fitosteroller; hücre büyümesi, gelişmesi ve farklılaşması gibi çeşitli biyolojik süreçte de görev alırlar. İzoprenoid biyosentez yolağı ile sentezlenen fitosteroller, bitki hormonlarının bir grubu olan brassinosteroidlerin (BRs) de öncül molekülleridir. Birçok enzimatik reaksiyon içeren biyosentez yolağında, kilit noktalarda kritik rol oynayan sterol metiltransferazlar nihai fitosterol konsantrasyonunun belirlenmesi açısından önem arz etmektedir. Bu çalışmanın amacı Türkiye'de yaygın olarak yetiştiriciliği yapılan dört farklı zeytin çeşidinin (Ayvalık, Gemlik, Memecik ve Gökçeada) genomunda *SMT* genlerini (*SMT1* ve *SMT2*) tanımlamak ve zeytin meyve olgunlaşması boyunca bu genlerin anlatımlarını analiz etmektir. Bu kapsamda SMT genlerinin referans protein dizileri model organizma *Arabidopsis thaliana* ve *Solanum lycopersicum* bitkisinden elde edilmiş olup biyoinformatik analizler ile zeytin genomunda aday gen bölgeleri belirlenmiştir. Elde edilen aday *OeSMT* gen dizilerine özgü primerler tasarlanmış ve gen anlatım çalışmaları gerçek zamanlı PZR çalışmaları ile yürütülmüştür. Daha sonra *OeSMT* genleri için klonlama çalışmaları yapılmış ve bu genlerin karşılaştırmalı analizleri gerçekleştirilmiştir. Elde edilen bulgulara göre *OeSMT1* geninin ifadesi meyve olgunlaşmasının son dönemlerinde artarken *OeSMT2* geninin ifadesinin meyve olgunlaşması boyunca aktif bir şekilde devam ettiği gözlemlenmiştir.

Ayrıca yapılan klonlama çalışmalarının sonucunda zeytin *SMT* genlerinin dizileri ilk kez ortaya çıkarılmıştır. Bu genlerin moleküler ölçekte karakterize edilmeleri fitosterol biyosentezinde önemli rolleri olduğu göz önüne alındığında, ileri moleküler ıslah çalışmalarına ışık tutacak niteliktedir. Elde edilen sonuçlar fitosterol içeriği yüksek zeytin çeşitlerinin tespit edilmesi ve geliştirilmesine kayda değer katkılar sağlayacaktır.

Anahtar Kelimeler: Fitosterol, Sterol metiltransferaz, Zeytin, *SMT1*, *SMT2*

ABSTRACT

MOLECULAR AND BIOINFORMATIC IDENTIFICATION OF TWO STEROL METHYLTRANSFERASES WHICH ARE INVOLVED IN PLANT STEROL BIOSYNTHESIS IN OLIVE (*Olea europaea* L.)

Kübra ÖZTÜRK

Çanakkale Onsekiz Mart University

School of Graduate Studies

Master of Science Thesis in Molecular Biology and Genetic

Advisor: Prof. Dr. Kemal Melih TAŞKIN

30/01/2023, 59

Plant phytochemicals known as phytosterols have recently become the focus of many studies in the scientific community due to their various benefits to human health. PSs, which are the basic building blocks of cell membranes in plants; are also involved in various biological processes such as cell growth, development, and differentiation. PSs synthesized by the isoprenoid biosynthesis pathway are also the precursor molecules of BRs, a group of plant hormones. In the biosynthesis pathway, which includes many enzymatic reactions, sterol methyltransferases, which play a critical role at key points, are important in terms of determining the final PS concentration. This study aims to identify *SMT* genes (SMT1 and SMT2) in the genome of four distinct olive cultivars (Ayvalık, Gemlik, Memecik, and Gökçeada) widely cultivated in Türkiye and to analyse the expressions of these genes during olive fruit ripening. In this context, reference protein sequences of *SMT* genes were obtained from the model organism *Arabidopsis thaliana* and *Solanum lycopersicum*, and candidate gene regions in the olive genome were determined by bioinformatics analysis. Target-specific primers for the obtained candidate *OeSMT* gene sequences were designed and gene expression studies were carried out with real-time PCR studies. Moreover, cloning studies of the *OeSMT* genes were performed in order to comparative analysis of these genes. According to the findings, it was observed that the expression of the *OeSMT1* gene elevated in the beginning stages of fruit maturation, while the expression of the *OeSMT2* gene was maintained actively throughout fruit maturation.

Furthermore, the sequences of the olive *SMT* genes were identified for the first time as a result of cloning studies. The outcomes of this research will make significant contributions to the identification and development of olive varieties with high PS content.

Keywords: Phytosterols, Olive, Sterol methyltransferases, *SMT1*, *SMT2*

TABLE OF CONTENTS

Page No

ETİK BEYAN/ PLAGIARISM DECLARATION…… i

ACKNOWLEDGEMENTS…… ii

ÖZET ……..…….…….. iii

ABSTRACT …….. v

TABLE OF CONTENTS……... vii

ABBREVIATIONS…….…….....……. x

LIST OF TABLES ...…….…. xi

LIST OF FIGURES……..……...…….….. xii

CHAPTER I 1

INTRODUCTION

1.1. Olive plant...…….……..… 1

1.2. Physiological functions of phytosterols in higher plants....……... 2

1.3. Diversity and chemical structures of phytosterols ……....…….. 3

1.4. Biosynthesis of phytosterols…….. 4

CHAPTER 2 7

PREVIOUS STUDIES

2.1. Olive phytosterol studies…….....…….…..... 9

2.2. Health-promoting effects of phytosterols ……...……...…...…… 11

CHAPTER 3 12

MATERIALS AND METHODS

3.1. Plant material....……..... 12

3.2. Total RNA Extraction....……...…….…..... 13

3.3 Determination of quality and quantity of RNAs…… 13

3.3.1. Agarose Gel Electrophoresis...…….……..…..….. 13

3.3.2. Preparation of 10X TAE buffer …….…… 14

3.3.3. Preparation of 1X TAE buffer …….…….. 14

3.3.4. Preparation of ethidium bromide solution ……. 14

3.3.5. Qubit fluorometric quantification ……. 14

3.4. DNAse treatment and cDNA synthesis ……...…….…..... 14

3.5. Bioinformatic analysis …….……...…….…..... 16

3.6. Comparative analysis of phytosterol genes....……...…..... 16

3.6.1. Primer designing……..…… 16

3.6.2. Gradient PCR reactions …….. 17

3.6.3. DNA extraction from agarose gel ……... 18

3.6.4. Competent cell preparation ……. 18

3.6.5. Ligation ……... 19

3.6.6. Transformation …… 19

3.6.7. Colony PCR …… 20

3.6.8. Plasmid isolation ……. 21

3.6.9. Plasmid restriction …….. 22

3.6.10. Sequence alignment and phylogenetic analysis …… 22

3.7. Selection of primers to use in gene expression studies ……. 23

3.8. Determination of primer efficiencies ……...……. 23

3.9. Gene expression analysis …….. 24

CHAPTER 4 27

RESULTS AND DISCUSSION

4.1. Plant materials ....……..…..... 27

4.2. RNA isolation and synthesis of cDNA ....…….…..... 28

4.3. Bioinformatic analysis …….. 30

4.4. Cloning and Comparative analysis of the full-length cDNA of *OeSMT* genes… 32

4.5. Sequence alignment and phylogenetic analysis of *OeSMTs* …… 38

4.6. Gene expression studies ……..….. 42

4.6.1. The efficiency of primers …….. 42

4.6.2. The expression studies of *OeSMT* genes in olive fruit tissue …… 47

CHAPTER 5 52

CONCLUSION

REFERENCES..……. 54

APPENDIX …….……. I

CV …….. IV

ABBREVIATIONS

FAO	Food and Agriculture Organization of the United Nations
TUBITAK	The Scientific and Technological Research Council Of Türkiye
BRs	Brassinosteroids
aa	Amino Acid
HMGR	3-hydroxy-3-methylglutaryl-CoA reductase
SQE	Squalene epoxidase
CAS	Cycloartenol synthase
cDNA	Complementary DNA
PCR	Polymerase chain reaction
Bp	Base pair
TAIR	The Arabidopsis Information Resource
Kb	Kilobase
UV	Ultraviolet
E. coli	*Escherichia coli*
$CaCl_2$	Calcium chloride
M	Molarity (Molar concentration)
mL	Millilitre
LDL	Low-density lipoprotein
LB	Luria-Bertani
ER	Endoplasmic reticulum
AdoMet	*S*-adenosyl-L-methionine
BLAST	Basic Local Alignment Search Tool

LIST OF TABLES

Table No	Table Name	Page No
Table 1	The harvest dates of olive fruit samples ……..	12
Table 2	Components of the DNase reactions……	14
Table 3	Components of cDNA RT mix ……	15
Table 4	Thermal cycler program for cDNA synthesis ……..……	15
Table 5	Gene cloning primers for *OeSMT* genes …….	16
Table 6	The components of gradient PCR ……...	17
Table 7	Gradient PCR thermal cycle ……	18
Table 8	Blunt-end ligation reaction components ……..	19
Table 9	Components of the restriction reactions ……..	22
Table 10	1:10 serial dilution of cDNAs ……	24
Table 11	Components of Real-time PCR reactions ……	25
Table 12	The RNA concentrations of olive oil samples for 8 ripening stages…….....	29
Table 13	Information on primers used in gene expression studies ….....	42

LIST OF FIGURES

Figure No	Figure Name	Page No
Figure 1	The purple-covered areas represent olive-growing regions in Türkiye……...	2
Figure 2	Chemical structure of cholesterol, cycloartenol, campesterol, *β*-sitosterol, and stigmasterol……	3
Figure 3	Biosynthetic pathway of phytosterols……	6
Figure 4	The ladder is composed of fourteen chromatography-purified individual DNA fragment …….	13
Figure 5	pCR™ – Blunt vector map……	21
Figure 6	qPCR plate layout …….	25
Figure 7	Thermal cycle of real-time PCR reactions ……...	26
Figure 8	The olive fruit samples which were used for RNA isolation……	28
Figure 9	Gel image of July 1, 2019 RNA samples of olive fruit tissues….	29
Figure 10	Phylogenetic tree for SMT protein sequences ……..	31
Figure 11	The candidate transcript sequences of the olive SMTs ……	32
Figure 12	Information on designed primers for *OeSMT* genes …….	33
Figure 13	The products of *OeSMT1* and *OeSMT2.2* after gradient PCR….	33
Figure 14	The products of *OeSMT2.1* after gradient PCR……	34
Figure 15	Reimaged *OeSMT1, OeSMT2.1*, and *OeSMT2.2* products after gel extraction ……	34
Figure 16	*E. coli* colonies incubated overnight in selective medium …...…	35

Figure 17	Colony PCR results of *OeSMT1* and *OeSMT2.2* …….……	35
Figure 18	Colony PCR results of *OeSMT2.1* ……...……	36
Figure 19	Plasmid digestion with double-cut EcoRI ……	37
Figure 20	Plasmid digestion of *OeSMT2.2*:pCR™-Blunt vector ….....	37
Figure 21	*OeSMT1* consensus sequences and assembled chromatogram sequences ……..	38
Figure 22	*OeSMT2.1* consensus sequences and assembled chromatogram sequences ……	39
Figure 23	*OeSMT2.2* consensus sequences and assembled chromatogram sequences ……..	39
Figure 24	Sequence alignment of OeSMT proteins with reference AtSMT protein sequences……...……	40
Figure 25	Phylogenetic tree for SMT transcripts ……..	41
Figure 26	The efficiency curve of SMT1 primer pair ……...	43
Figure 27	The efficiency curve of SMT1.2 primer pair ……	44
Figure 28	The efficiency curve of SMT2 primer pair ……...	45
Figure 29	The efficiency curve of SMT2.1 primer pair ……	46
Figure 30	Melt curve analysis of *OeSMT* genes and housekeeping genes ...	47
Figure 31	Gene expression results of the *OeSMT1*……	48
Figure 32	Gene expression results of the *OeSMT1.2* ……	49
Figure 33	Gene expression results of the *OeSMT2*……	50
Figure 34	Gene expression results of the *OeSMT2.1*……	51

CHAPTER I

INTRODUCTION

1.1. Olive plant

Olea europaea L. is one of 30 species in the genus *Olea* (Bracci et al., 2011). The fruit of the olive tree is a drupe with a blackish-violet hue when completely ripe in late fall. Cultivated olive trees are primarily self- or cross-pollinated by wind so as a result of high rate of cross-pollination there are numerous olive cultivars that exhibit different sizes, shapes, flavours, and oil contents (Hatzopoulos et al., 2002). It is widely known that a cold, rainy winter is necessary for olives to go into dormancy to differentiate their flower buds and that a hot, dry summer follows to produce fruit with a high oil content (Ramos et al., 2018). Considering olive oil's beneficial properties for human health olive becomes an important crop. Globally, about 23 million tons of green and black table olives and 3.4 million tons of oil are currently in production. 95 % percent of the total production is made in the Mediterranean region, with Spain and Italy serving as the two largest producing nations (FAOSTAT, 2020). According to the Food and Agriculture Organization of the United Nations (FAO), Türkiye produces an average of 1.738.680 tons of olives annually (FAO, 2021). The Aegean region is the territory where olive cultivation is most intensive (Figure 1). Among the priority provinces in olive production; Aydın, İzmir, Muğla, Manisa, Balıkesir, Çanakkale, Mersin and Hatay are included.

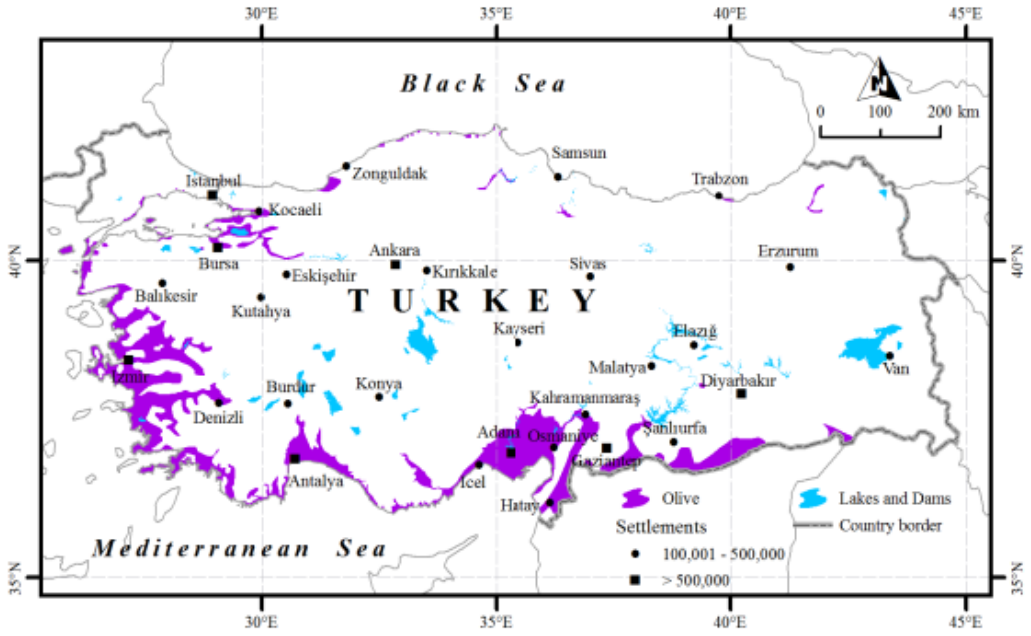

Figure 1. The purple-covered areas represent olive-growing regions in Türkiye (Efe et al., 2013).

1.2. Physiological functions of phytosterols in higher plants

PSs, which are isoprenoid-derived molecules, are well-known as the essential structural elements of the cell membrane in higher plants. With their action on organizing fatty acid chains, they alter the state of membranes to maintain fluidity and permeability (Brown, 1998). In particular, stigmasterol, campesterol, and sitosterol act in membranes to reduce the fatty acid chain mobility. With any temperature fluctuations, PSs increase membrane cohesiveness to make it more resistant to temperature shock (Dufourc, 2008). In general, plant cells respond to several biotic and abiotic stresses by changing the PS composition of the plasma membrane (Valitova et al., 2016). Hence, it is possible to conclude that PSs are effective in response to stress conditions. Through interacting with phospholipids and sphingolipids to generate specific lipid microdomains (lipid rafts) in the membrane, PSs have a direct role in the signal transduction (Mongrand et al., 2004). Moreover, PSs are requisite for cellular differentiation and proliferation. It was proven the production of PS increases significantly throughout seed germination, and accumulated sterols in seeds serve as a reservoir for the germination (Piironen et al., 2000). Finally, PSs are involved in the biosynthesis of BRs as a precursor so they participate in regulation of plant growth and development (Choe et al., 1999) .

1.3. Chemical structures and diversity of phytosterols

PSs are a chemical form of triterpenes with a four-ring structure known as the perhydrocyclopentanophenanthrene ring system (Mohammadi et al., 2020). They have a similar structural basis to cholesterol by consisting of hydrated phenanthrene (A-, B-, and C-ring) a cyclopentane (D-ring), and a variable alkyl side chain at the C-17 position (Figure 2). In general, plant sterols are found in the form of free sterols, sterol esters, sterol glycosides, and acyl sterol glycosides. The term ‘’free sterols’’ refers to possessing no linkages between these sterols and any other chemical constructures. The free sterols structure can be characterized by an unbounded β-hydroxyl group at the C3 position, one or multiple double bonds in the B ring, and in the side chain (Figure 2) (Feng et al., 2021).

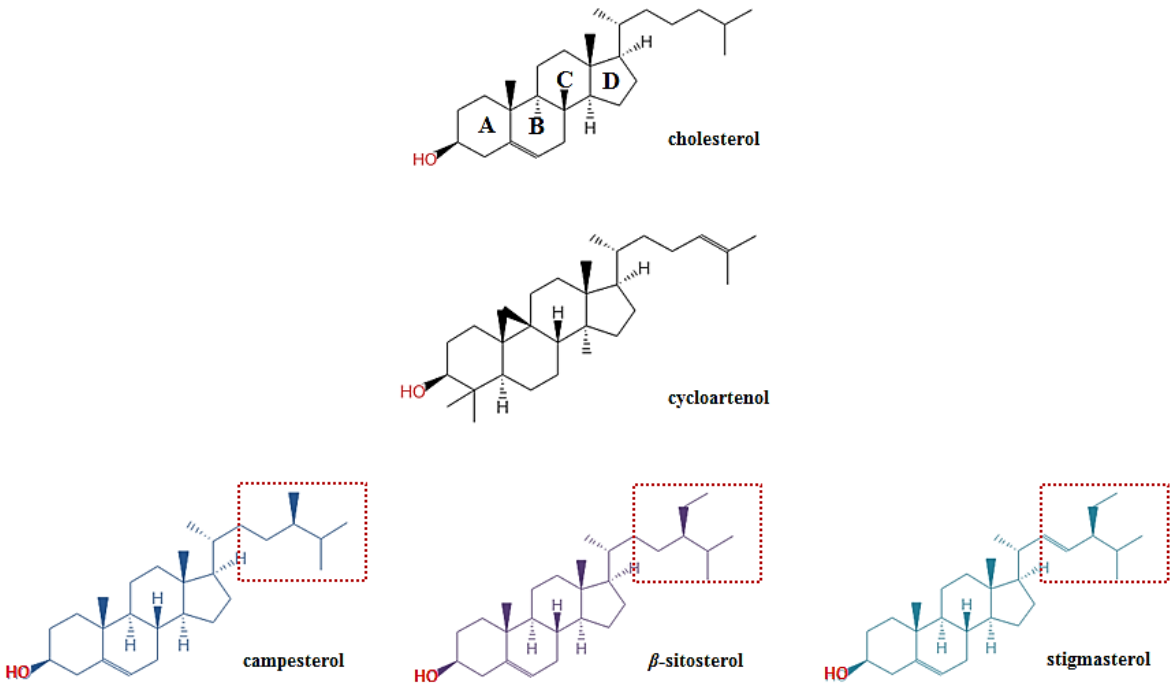

Figure 2. Chemical structure of cholesterol, cycloartenol, campesterol, *β*-sitosterol, and stigmasterol. Red rectangles represent the chemical differences between campesterol, β-sitosterol, and stigmasterol.

According to the presence and quantity of methyl substituents on C4, PSs can be categorized into three classes: 4, 4-dimethyl sterols, 4α-methyl sterols, and 4-desmethyl sterols. In the plant sterols biosynthetic pathway, 4,4-dimethyl sterols (cycloartenol and cycloartanol), and 4α-methyl sterols are the precursor molecules of 4-desmethyl sterols (*β*-sitosterol, stigmasterol, campesterol, and brassicasterol) (Moreau et al., 2002). 4-desmethyl sterols are the most abundant of the more than 250 different PS types that have been reported in plants up to now (Nes, 2011). 4-desmethyl sterols can be categorized into 24-methyl and 24-ethylsterols based on the presence of methyl or an ethyl group at the C24 position of the side chain. At its 24th carbon, campesterol only contains one methyl group. Similar to *β*-sitosterol, stigmasterol includes an ethyl group at the C24 position, but it also has an unsaturated double bond at the C-22 position (Benveniste, 2004).

1.4. Biosynthesis of phytosterols

In plants, the PSs are synthesized in the endoplasmic reticulum (ER) via the isoprenoid biosynthetic pathway. The entire biosynthetic pathway can be addressed in three steps. The pre-squalene section of the pathway is referred to as the initial step and the conversion of acetyl CoA to 2.3-oxidosqualene occur in three reactions by the catalysis of various enzymes (Figure 3). 3-hydroxy-3-methylglutaryl-CoA reductase (HMGR), catalyzes the synthesis of mevalonate and this enzyme is considered a rate-limiting enzyme of plant sterol biosynthesis (Valitova et al., 2016). In the second section of biosynthesis, the squalene epoxidase (SQE) catalyzes squalene cyclization to form cyclic triterpene skeletons and the following cycloartenol synthase (CAS) catalyzes the reaction of formation cycloartenol in plants. Once cycloartenol is formed biosynthesis is divided into two different paths. At this point, the cycloartenol is transformed into cholesterol by sterol side chain reductase 2 (SSR2) or PSs by C24-sterol methyltransferase 1 (SMT1). S-adenosyl-L-methionine-dependent C24-sterol methyltransferase (EC 2.1.1.41) has a key role in PS biosynthesis via catalyzation of C24 methylation. SMT is an integral protein found in the ER and two distinct forms of SMT (SMT1 and SMT2) exhibiting differing substrate specificities, end products, and kinetic reactions exist (Bouvier-Navé et al., 1997; Schaeffer et al., 2001).

SMT1 catalyzes the methylation of cycloartenol and leads to the formation of 24-methylene cycloartenol. Once more, the biosynthetic pathway divides into two branches in this step.

SMT2 converts the 24-methylene cycloartenol to 24-methylene lophenol and the 24-ethylsterols (β-sitosterol and stigmasterol) are produced consecutively as the final products. Four enzymatic steps in the other branch of the pathway resulting in the conversion of 24-methylene lophenol to campesterol (Figure 3) (Miras-Moreno et al., 2016). In the model organism *Arabidopsis thaliana* two *SMT2* isoforms (*SMT2* and *SMT3*) are found. The proportion of 24-methyl- and 24-ethylsterols depends on *SMT2* activity. Hence, it can be said that *SMT2* activity is closely related to plant growth and development (Schaller, 2003).

The goal of this study is to identify the *SMT* genes participating in the essential steps of PS synthesis in the olive genome and to assess the levels of gene expression during the development of the olive fruit.

Overall, in the extent of this thesis;

- Olive fruit samples were taken from Ayvalık, Gemlik, Memecik, and Gökçeada cultivars at 8 consecutive ripening stages, and RNA was isolated from these tissues.
- Bioinformatic analysis was performed to identify *SMT* genes in the olive genome. Respectively candidate olive *SMT* sequences were determined and appropriate primers were designed for further gene expression and comparative analysis.
- Expressions of *SMT* genes that have crucial role in the PS biosynthesis pathway were determined by quantitative Real-Time PCR method by using 3 technical and 3 biological replicates and were analysed with the comparative Ct method.
- *OeSMT* genes were cloned. Following the cloning procedure, the sequences belonging to *SMT* genes were revealed in *Olea europaea* L. genome.

Gene expression and sequencing data of *OeSMT* genes obtained with this study provide important data to better understand the PS biosynthesis process in olive cultivars. Hence these molecular data will be useful for the selection of cultivars with high PS content in olive species.

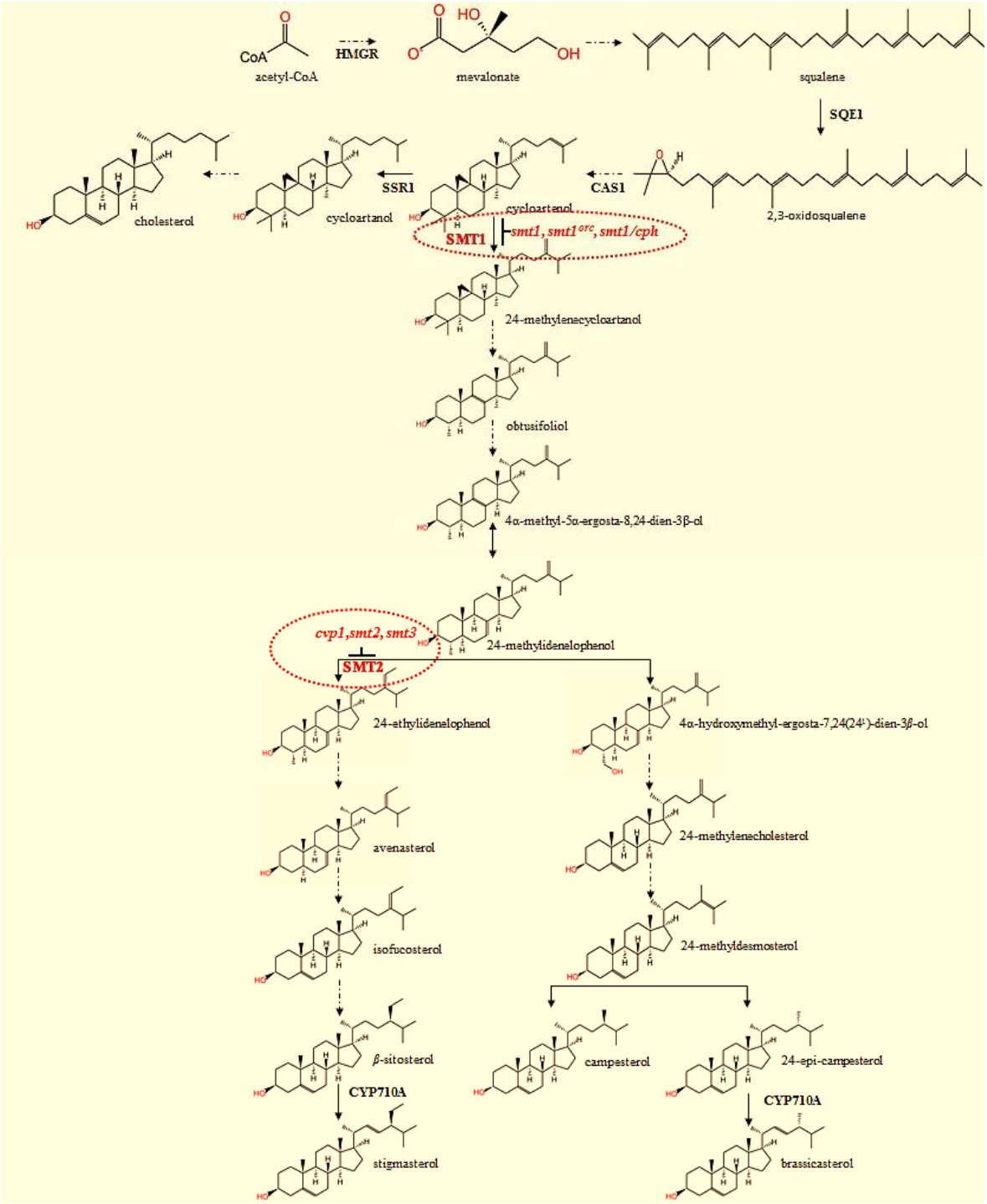

Figure 3. Biosynthetic pathway of phytosterols. Only main compounds and enzymes were depicted in the figure. Dashed arrows represent multiple steps of biosynthesis. Red circles represent *SMT* genes and mutant lines.

CHAPTER 2
PREVIOUS STUDIES

PSs serve as one of the fundamental building component of eukaryotic plasma membranes due to maintaining fluidity and permeability (Hartmann, 1998). Furthermore, they have important roles in many cellular processes including stress response, regulation of various physiological activities, and cell division (Piironen et al., 2000). In addition, BRs, which are crucial hormones for plants, are also synthesized through the PS biosynthetic pathway (Li et al., 1996). Plants contain numerous types of sterols, over 250, however, the majority of the total amount is comprised of *β*-sitosterol, stigmasterol, and campesterol (Nes, 2011). Depending on their species and cell types, vascular plants include different proportions of 24-alkyl-Δ^5-sterol (Schaller et al., 1998). The final 24-methyl and 24-ethyl sterol ratio, which is critical for usual plant development, is adjusted through the sterol side chain C24-alkylation reactions (Schaeffer et al., 2001). Two different SMTs are in charge of adding exocyclic carbon atoms from S-adenosyl methionine to acceptor compounds at the most pivotal point of PS biosynthesis (Figure 3) (Nakamoto et al., 2015). SMTs, therefore, arouse intense attention in the research of PS biosynthesis.

SMTs have been isolated and cloned from fungi, protozoa, and a variety of higher plants including *Arabidopsis thaliana* (Diener et al., 2000), *Glycine max* (Neelakandan et al., 2009), *Nicotiana tabacum*, *Oryza sativa* (Bouvier-Navé et al., 1998), and *Zea mays* (Grebenok et al., 1997). SMTs are integral membrane proteins localized to the ER in higher plants and they have the quaternary structure of four identical subunits each containing a single active side for sterol and *S*-adenosyl-L-methionine (AdoMet) (Nes, 2000). *SMT* genes can be grouped into 2 families, *SMT1* and *SMT2* based on the examination of amino acid sequences of the cDNAs in various studies (Bouvier-Navé et al., 1998). *SMT1* and *SMT2* genes are responsible for the encoding of two separate enzymes which have distinct substrate specificities and enzyme kinetics. Both SMT enzymes maintain carbon flux through the biosynthesis pathway via methylation of precursor sterols, so they are of great importance for PS biosynthesis.

The primary methylation occurs with the action of the SMT1 enzyme (EC 2.1.1.142) which is encoded by the *SMT1* gene. When cycloartenol is methylated with SMT1 enzyme catalyzation biosynthesis continues in direction of the plant sterol synthesis hence SMT1 activation affects the total concentration of PSs. The methylation of 24-methylene lophenol occurs with the action of the SMT2 enzyme (EC 2.1.1.143) which is encoded by the *SMT2* genes. At this point of biosynthesis, action of the SMT2 enzyme determines the balance between C24-ethylsterols and C24-methylsterols (Nes et al., 2003; Schaeffer et al., 2001). In the study upon *Arabidopsis smt1* mutants, an aberrant phenotype was observed in absence of *SMT1* gene expression. Low fertility with stunted siliques, deficient growth with shorter petioles and smaller, rounder leaves, increased calcium tenderness of the *Arabidopsis* root, and aberrant embryo morphogenesis was noticed. Furthermore, compared to wild-type *Arabidopsis* plants, *smt1* mutants exhibited an altered ratio between cholesterol and C-24 alkylated sterols concentration. Moreover, various previous studies upon the *Arabidopsis smt1/cph* and *smt1*^{orc} mutants show that deficiency of *SMT1* gene activity causes unaccomplished cell wall constructions via insufficiency in cellulose deposition and defective auxin efflux via distributed PIN1-PIN3 protein placement in the membrane (Schrick et al., 2004).

SMT2 activity also regulates the ultimate proportion of total sterol and thus plant growth (Schaller et al., 1998). The overexpression of SMT2.1 in *Arabidopsis* plants shifted the biosynthetic pathway to the sitosterol synthesis direction so reduced stature and growths were observed in these plants. However, exogenous supplementation of BRs provided the recovery of the phenotypes of these plants. In the same study co-suppression of *SMT2.1* resulted in a shift in the biosynthetic pathway in the direction of the campesterol segment and plants were characterized by pleiotropic deficiencies such as poor growth, excessive branching and low fertility. Surprisingly this time the morphological defects of these plants were not rescued by BRs supplementation (Schaeffer et al., 2001). In the other research upon *Arabidopsis cvp* mutants, abnormal cotyledon vascular patterning, aberrant floral development, and reduced stature were observed (F. M. Carland et al., 2002).

Furthermore, compared to *cvp1* mutants more remarkable abnormalities were observed in *cvp1 smt3* double mutant plants. Besides various unusual features of growth, poor root development, and deficient apical dominance were reported. These defects of the phenotype were associated with significant changes in the ratio of particular sterols without significant changes in BR profiles (F. Carland et al., 2010). Moreover, cell division plane determination, directional auxin transport, and polar expansion were affected by the absence of *SMT2* expression in the *Arabidopsis* mutant lines (*smt2, smt3*) (Nakamoto et al., 2015).

Olive phytosterol studies

There are numerous natural PS sources, and individuals consume plant sterols in their cereal, fruits, and edible vegetable oils. Vegetable oils rank highest in PS content (150–1,231 mg/100 g), followed by legumes, nuts, and cereals. According to the research on the PS content of 14 different vegetable oils, the total PS content varied between 142.64 and 1891.82 mg/100 g in plant oils. While rice bran oil, corn oil, and rapeseed oil had a higher PS content, it was reported that olive oil ranked 9th with containing 288.02 mg/100 g of PS (Yang et al., 2019).

In the research on the PS composition of rapeseed and olive oil, 19 novel rapeseed cultivars and 21 distinct olive cultivars growing in Northwest Türkiye, were compared in terms of their PS content. As a result, it was detected that the total PS content of olive oil ranged between 1.29 and 2.38 g/kg in different olive cultivars whereas compared to the others the Gökçeada cultivar contains the highest level of PS (Gül & Şeker, 2006). Similarly, the PS content of virgin olive oil of three significant olive cultivars in Italy (Carolea, Cassanese, and Coratina) was investigated on two separate harvesting dates (October and November). While higher PS content was observed in the samples harvested in November, it was noticed that the Coratina species had the richest PS content (Sivakumar et al., 2006).

The correlation between sterol accumulation and olive fruit ripening was investigated. Fruit samples of Picual and Arbequina were harvested at regular intervals for 4 months and the PS content of olive oil was detected. The PS content of olive fruits increased from September to December. Especially, the sitosterol level decreased from September to November on the contrary Δ-5avenasterol level increased in the same timeline. Overall, while considerable differences were observed in the PS content between September and November however no notable changes were detected between November and December (Fernández-Cuesta et al., 2013).

The total PS content of forty-three olive cultivars from 11 different countries of cultivars' origin was compared in the large-scale research. In this study, which included two cultivars named "San Sun Tuzcamalık" and "Beyaz Yağlık" from Türkiye, it was determined that the total sterol content ranged between 855 and 2185 mg/kg. In addition, it has been stated that PSs that are predominantly found in olive oil (β-sitosterol, Δ^5-avenasterol, campesterol, and stigmasterol) exhibit high variability among the cultivars, and this variability is due to high genetic factors (Kyçyk et al., 2016). In a different research, both the fatty acid and PS composition of Kilis Yağlık and Nizip Yağlık cultivars were analysed. Comparative analysis of samples of olive fruit collected from 34 separate territories was performed. Among the studied 7 different type of PSs, β-sitosterol, Δ^5-avenasterol and campesterol were most abundantly found in both olive oil samples. Consequently, the only evident difference between the two cultivars was that Nizip Yağlık had a higher amount of 7-stigmasterol than Kilis Yağlık (Ozkan et al., 2017).

The correlation between the PS content of olive and early fruit-flower development was examined. Additionally the gene expression of *OeCYP51* and *OeSMT2* genes were examined in this study. They demonstrated that the expression of these genes increased in olive floral tissues concurrently with the raise in the concentration of total sterol and displayed different expression patterns during the early stages of fruit maturation. Furthermore, the correlation between sitosterol and BRs was also investigated by supplementation of 24-epibrassinolide and brassinazole. Early tissue development was observed in olive fruit after treatment with 24-epibrassinolide.

Moreover sitosterol content and *OeSMT2* gene expression were increased whereas *OeCYP51* gene expression decreased with the 24-epibrassinolide treatment. Conversely, an inverse effect was observed when BR biosynthesis was inhibited with brassinazole treatment (Inês et al., 2019).

Health-promoting effects of phytosterols

In the past decades, PSs are attracting the attention of the global market due to their beneficial impacts on metabolism and human health. Notably, it has been approved that the regular daily consumption of phytosterol-enhanced foods diminishes LDL cholesterol and lower the risk of cardiovascular disease by the US Food and Drug Administration, the European Food Safety Authority. Various clinical research on hypercholesterolemic subjects revealed that consuming 1.5-3 g of plant sterols diurnally reduces the intestinal absorption of cholesterol thus, lowering serum low-density lipoprotein (LDL) cholesterol levels by 8% to 15% (Orem et al., 2017; Quílez et al., 2003). In addition to the reputed cardiovascular benefits of PSs, their anticancer effects have also become the focal point of numerous studies. Findings regarding the anticancer impact of PSs rely on several mechanisms including acting as antioxidants and regulating the proliferation and apoptosis of tumour cells for numerous cancer types (Bouic et al., 1997; Shenouda et al., 2007). In addition to all these health-promoting effects of PSs the anti-hypertensive, anti-obesity, and anti-inflammatory properties also make them very intriguing dietary supplements for human health (Nattagh-eshtivani, 2022)

CHAPTER 3
MATERIALS AND METHODS

3.1. Plant material

Three olive cultivars (*O. europaea* L.) were provided from the Edremit Olive Production, Training and Gene Center were studied: Ayvalık, Memecik, and Gemlik. Simultaneously, the Gökçeada variety was obtained from the Gökçeada district agriculture directorate. Fruit samples were harvested between 1 October-15 December 2019 in 15-day intervals at eight different ripening stages (Table 1). Ripening stages of olive fruits were determined according to maturation index of olive fruits. Harvested olive fruits were immediately frozen in liquid nitrogen until they reached to the laboratory. All fruit samples were stored -80 ºC until use.

Table 1

The harvest dates of olive fruit samples

Olive fruit ripening stages	Harvest Date
1st	July 1,2019
2nd	July 15,2019
3th	August 1,2019
4th	August 15,2019
5th	September 1,2019
6th	September 15,2019
7th	October 1,2019
8th	October 15,2019

3.2. Total RNA Extraction

Total RNA of olive fruits was extracted by using Trizol (TRIzol™ Reagent-Invitrogen - 15596018) and RNA isolation kit (RNA Mini Kit – Invitrogen – 12183018A) according to the manufacturer's instructions. Before the RNA isolation mortars, grinds, spatulas, and forceps were treated with DEPC solution (Himedia, MB076) for overnight and then sterilized with autoclave (121^{o}C, 15 min). The olive tissues were ground with pre-cooled mortars in liquid nitrogen and after the removal of endocarp tissue, 100 mg mesocarp tissue of olive fruits was treated with 1 mL of Trizol solution. Isolation of RNA was continued with the RNA isolation kit according to the manufacturer's instructions and isolated RNA was stored at –80 ^{o}C until use.

3.3. Determination of quality and quantity of RNAs

The integrity of isolated RNA was visualized with 1% agarose gel electrophoresis and the concentrations were measured with a Qubit 2.0 fluorometer (Invitrogen, Q32866). Any possible DNA contamination was removed by using DNAse I (Fisher Scientfic – USA).

3.3.1. Agarose Gel Electrophoresis

In this research, RNA, and DNA samples were visualized by 1% agarose gel electrophoresis. All samples were loaded into wells after mixing with 6X loading dye and as a determinant, 1 kb GeneRuler DNA Ladder (Thermo Scientific™, SM0311) was used (Figure 4). Finally, the electric field was applied for adequate time to separate the molecules and the agarose gel was visualized under ultraviolet (UV) light.

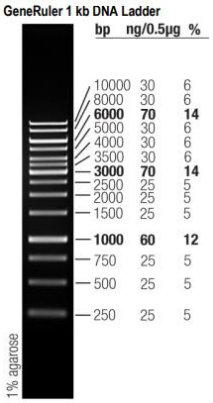

Figure 4. The ladder is composed of fourteen chromatography-purified individual DNA fragments (in base pairs).

3.3.2. Preparation of 10X TAE buffer

To prepare 10X TAE buffer 48.44 g of Tris base and 3.72 g of EDTA were dissolved into 900 mL dH_2O and pH was adjusted to 8 with acetic acid (11.4 mL). The final volume of buffer was completed to 1 L with dH_2O. Prepared 10X TAE buffer was autoclaved (121 ºC, 15 min) and stored at room temperature.

3.3.3. Preparation of 1X TAE buffer

1X TAE buffer was prepared by 10:1 dilution of 10X TAE buffer (100 mL of 10X TAE buffer, 900 mL of dH_2O).

3.3.4. Preparation of ethidium bromide solution

EtBr was added into agarose gel right before the gel electrophoresis. Stock solution of EtBr was prepared by dissolving 100 mg of EtBr into 10 mL dH_2O.

3.3.5. Qubit fluorometric quantification

The concentrations of RNAs were measured with Qubit fluorometer device (Invitrogen, Q32866) by the instructions of the device. The concentration of the RNA sample was measured by using Qubit™ RNA Broad Range (BR) Assay Kit (Invitrogen, Q10211) in the directions of the manufacturer.

3.4. DNAse treatment and cDNA synthesis

To avoid DNA contamination, DNAse I (4368814; Applied Biosystems) treatment was carried out once RNA concentrations were measured. 1000 ng of RNA from each sample was used for cDNA synthesis. All reaction were prepared in a total volume of 10 µl (Table 2) and incubated at 37 ºC for 30 min.

Table 2

Components of the DNase reactions

Components	Volume	Final concentration
10X reaction buffer	1 µL	1 x
RNA	1000 ng	100 ng / µL
DNase I (1 u/µL)	1 µL	0.1 u / µL
Nuclease-free H_2O	Complete to 10 µL	-
Final volume	10 µL	-

1 µl of EDTA (50 mM), 2 µl of random primers, and 0.8 µl of dNTP mix were added to the reactions and DNAse I was inactivated at 65 °C for 10 min. Afterward, the High-Capacity cDNA Reverse Transcription Kit (High-Capacity cDNA Reverse Transcription Kit – 4374967) was used for cDNA synthesis. cDNA RT mixes were prepared for each reaction (Table 3) and added into reaction tubes.

Table 3

Components of cDNA RT mix

Components	Volume
10X RT buffer	2 µL
Reverse transcriptase	1 unit
Nuclease-free H_2O	3.2 µL
Total volume	6.2 µL

cDNA synthesis was completed using a thermal cycler (Biorad PTC200) and recommended program (Table 4) for High Capacity cDNA Reverse Transcription Kits. Synthesized cDNAs were stored at 4 ºC for short-term storage.

Table 4

Thermal cycler program for cDNA synthesis

Step	Temperature (ºC)	Time (min)
1	25	10
2	37	120
3	85	5
4	4	∞

3.5. Bioinformatic analysis

The existing databases were used to investigate the structures of *SMTs* genes in olive genome. With this purpose *Olea europaea* var. *Sylvestris* genome data was used. The genome, transcriptome, and proteome data of Sylvestris were downloaded from NCBI (National Center for Biotechnology Information) were added as a database into Geneious v.8.1 software. Reference protein sequences of these genes were obtained from model organisms such as *A. thaliana* and *S. lycopersicum* through The Arabidopsis Information Resource (TAIR) and NCBI databases were used as queries in the BLAST (Basic Local Alignment Search Tool) against to olive protein data. The resulting sequences were used to plot a UPGMA phylogenetic tree.

3.6. Comparative analysis of phytosterol genes

3.6.1. Primer designing

Cloning primers were designed with the selected olive *SMT* transcripts by using Geneious v.8.1 software (Table 5). The following criteria were considered during primer designing: Tm value was optimum 60 ℃, and Tm difference between primers was at most 1°C.

Table 5

Gene cloning primers for *OeSMT* genes

Gene name	Primer name	Sequence of primer	Expected base pair
SMT 1	SMT1_F	5’ TCTGAAGGCTCAATTTGACAGC 3’	702 bp
	SMT1_R	5’ AATGGCCTTCACCAGTCCTC 3’	
SMT 2.1	SMT 2.1_F	5’ GTCGTTTTTCCGGAGACCCA 3’	954 bp
	SMT 2.1_R	5’ TGCGATTTTCCAGGAACGGA 3’	
SMT 2.2	SMT 2.2_F	5’ CCACACCAACCCTAGACACA 3’	1266 bp
	SMT 2.2_R	5’ AGGAAGGAAATCAAGACTGCAAA 3’	

3.6.2. Gradient PCR reactions

PCR reactions were performed to obtain the required amplicons of *SMT* genes with the High Fidelity DNA Polymerase (Thermo Scientific, F530L) enzyme which has a low error rate via its proofreading function. Furthermore, this enzyme was used to amplify the products with the blunt end which was necessary for ligation with the pCR™-Blunt vector. PCR reactions were assembled with the components given below (Table 6).

Table 6

The components of gradient PCR

Components	Volume	Final concentration
5X High Fidelity PCR Buffer	5 µL	1X 10mM
dNTP mix	0,5 µL	200 µM
10µM Reverse Primer	1 µL	0,4 µM
10µM Forward Primer	1 µL	0,4 µM
Template cDNA	1 µL	-
High Fidelity PCR Enzyme Mix	0,25 µL	0,02 u/µL
Nuclease-free H_2O	16,25 µL	-

Gradient PCR was performed to obtain optimal annealing temperature for SMT primers, with convenient thermal cycling conditions (Table 7). Different annealing temperatures were applied at the temperature range of 54-60 °C.

Table 7

Gradient PCR thermal cycle

Cycle step	Temperature	Time	Cycle
Initial Denaturation	98°C	30 s	1
Denaturation	98°C	5–10 s	25–35
Annealing	54-60°C	30 s	
Extension	72°C	1 min	
Final extension	72°C	10 min	1

3.6.3. DNA extraction from agarose gel

PCR products were assessed by visualizing with 1% agarose gel electrophoresis under a UV light source. The correct DNA bands were extracted from gel by using PureLink® Quick Gel Extraction Kit (Invitrogen, K2100-12) according to the manufacturer's instructions. Extracted PCR products were visualized by 1% agarose gel electrophoresis. Concentrations of PCR products were measured with NanoPhotometer® P-Class P330 device.

3.6.4. Competent cell preparation

Cloning studies have proceeded with the *Escherichia coli* (*E. coli*) DH10B strain. Frozen stock of *E. coli* cells was inoculated into 50 mL LB (Luria-Bertani) broth medium (0.5 g Bacto-tryptone, 0.25 g yeast extract, 0.5 g NaCl) at 37 °C for overnight with shaking speed 130 rpm. On the following day, bacteria taken from the overnight media culture were streaked on the LB agar plate using a sterile inoculation loop with the aim of obtaining isolated single colonies, and plates were incubated again for overnight at 37 °C without shaking. The next day an isolated single colony was selected and inoculated into 50 mL LB broth by using a sterile loop then incubated with aerobic conditions at 37 °C, 130 rpm for overnight. Cloning studies of *OeSMT* genes proceeded with these overnight cultures. Next morning 500 µL of overnight culture was inoculated into 50 mL fresh LB broth media.

Excess amount of bacteria culture was stored in the 50 % glycerol suspension at -80 °C for future usage. OD value was measured until OD_{600} reaches to 0.3-0.4 with spectrophotometer. When *E. coli* cells grow to log phase, competent cells were prepared by using the calcium chloride ($CaCl_2$) followed by a heat-shock application.

3.6.5. Ligation

Ligation reactions were processed with T4 DNA Ligase (EL0011, Thermo Scientific™) and pCR™-Blunt vector (Zero Blunt® PCR Cloning Kit, K270020, Thermo Fischer). Extracted PCR products were ligated with pCR™-Blunt vector according to the manufacturer's instructions. The ligation reactions were prepared separately for each gene in a total volume of 20 µL (Table 8) and incubated at room temperature for 90 min. Prepared reactions were stored at -20 ºC until transformation.

Table 8

Blunt-end ligation reaction components

Ligation components	Volume
10X T4 DNA ligase buffer	2 µL
50% PEG solution	2 µL
T4 DNA ligase	1 µL
pCR™-Blunt vector	20-100 ng
Insert DNA	1:1 to 5:1 molar ratio over vector
Nuclease-free H_2O	9 µL
Total volume	20 µL

3.6.6. Transformation

After the incubation of ligation reactions, heat-shock transformation method was used to introduce plasmid DNA into competent *E. coli* cells. 20 µL of ligation suspension was mixed with 200 µL of competent cell suspension in a 1.5 mL microcentrifuge tube and incubated on ice for 30 min. To insert the plasmids into competent *E. coli* cells, tubes were submerged in a water bath for 90 s at 42 °C without shaking and incubated in the ice for 2 min immediately. Then 800 µL of SOC medium (%0. 5 Yeast Extract, %2 Tryptone, 10 mM NaCl, 2.5 mM KCl, 10 mM $MgCl_2$, 10 mM $MgSO_4$, 20 mM Glucose) was added onto transformed cell suspension. Transformed *E. coli* cells were incubated at 37 °C for 90 min with shaking gently.

At the end of incubation outgrowth culture was spread as three different dilutions (100, 150, and 200 µL) to LB plates supplemented with 50 µg/mL Kanamycin for selection. The cultures were incubated at 37 °C for overnight and colony growth was observed the next day.

3.6.7. Colony PCR

On the following day, the accomplishment of transformation was verified with colony PCR. For this purpose, colonies were chosen from petri dishes that had been cultured overnight in LB solid medium containing Kanamycin (50 µg/mL). With the use of a sterile loop, small amount of cells was collected from these colonies and suspended in 50 µL of nuclease-free water and this suspended cell solution was used as a template for colony PCR reactions. All reactions were prepared by using Phusion High Fidelity DNA Polymerase (Thermo Scientific, F530L) and M13 primers (Table 6 and Table 7). M13 primer binding sites on the vectors used in this project are depicted in Figure 5. PCR products were visualized with UV light after 1% agarose gel electrophoresis. The colonies which have the correct size plasmids were inoculated into 50 µg/mL Kanamycin contained 50 mL LB medium and incubated at 37 °C for overnight.

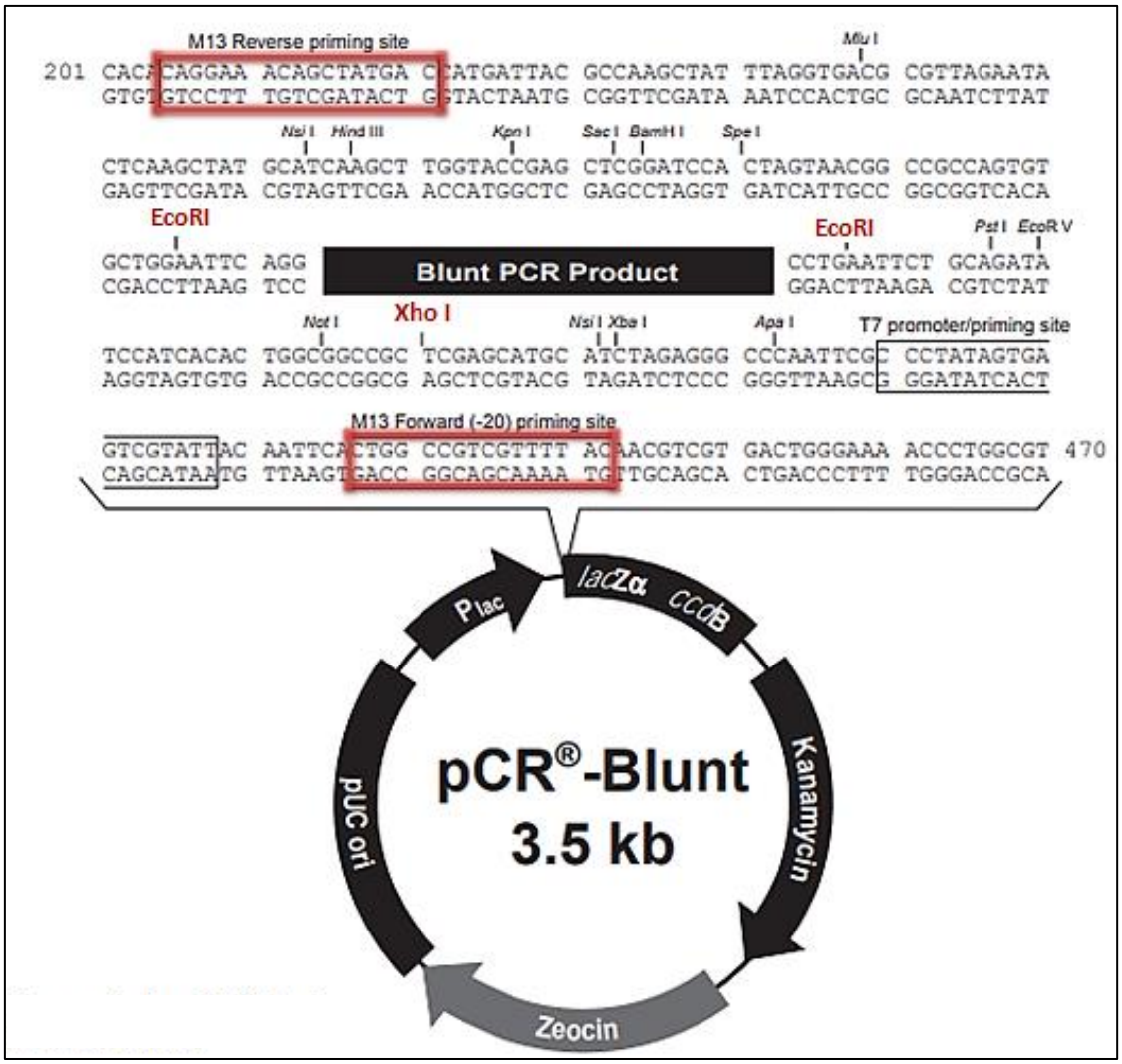

Figure 5. pCR™ – Blunt vector map. The figure contains restriction sites of EcoRI and XhoI enzymes, and M13 primers binding sites.

3.6.8. Plasmid isolation

Plasmid isolation was performed with GeneJET Plasmid Miniprep Kit (Thermo Scientific™, K0503) according to the manufacturer's instructions. The isolated plasmid DNAs were stored at -20°C.

3.6.9. Plasmid restriction

Isolated plasmids were restricted from two sites of transformed PCR product by using FastDigest EcoRI (FD0274, Thermo Scientific™) and only one region of plasmid by using FastDigest XhoI (FD0694, Thermo Scientific™). The cleavage sites of enzymes were shown in Figure 5. All reaction mixtures were prepared at room temperature in the order of the indicated Table 9 and then incubated at 37 ºC for 30 min. Finally, restriction enzymes were inactivated with incubation at 80 ºC for 5 min. Restricted plasmids were visualized with UV light after 1% agarose gel electrophoresis and the transformation of correct products was confirmed.

Table 9

Components of the restriction reactions

Component	Volume
Nuclease-free water	15 µl
10X FastDigest® buffer	2 µl
Plasmid DNA	2 µl (up to 1 µg)
FastDigest® enzyme	1 µl
Total volume	**20 µl**

3.6.10. Sequence alignment and phylogenetic analysis

The PCR products of *SMTs* genes, which play a key role in PS biosynthesis in olives, were transferred into the *E. coli* cells with pCR™-Blunt vector. After restriction enzyme confirmation, the nucleotide sequences of olive *SMTs* genes were revealed by a sequencing service (MEDSANTEK, Türkiye) through the Sanger method. The sequencing files (ab1) were analysed by the Geneious v.8.1 software. Firstly, the quality scores of chromatogram sequences were checked and the poor-quality regions in the 5'end and 3' end of each sequence were trimmed out with a 0.05 error probability cut-off value. All high-quality chromatogram sequences were assembled and mapped to reference sequences for each *SMT* gene then olive SMT protein sequences were obtained from the deduced consensus sequences.

The similarity between the deduced olive protein sequences and reference *A. thaliana* sequences was searched with the MUSCLE alignment. Moreover, conserved motifs were investigated in deduced protein sequences. Finally, consensus sequences of olive *SMTs* were searched by BLASTn program against other plant species in the NCBI database. The neighbor-joining method was used for phylogenetic tree analysis.

3.7. Selection of primers to use in gene expression studies

The primers to be used in gene expression studies were selected by using Geneious v.8.1 software. The *A. thaliana* reference protein sequences of *SMT* genes were obtained from TAIR and BLASTp analyses were performed against to *Olea europaea* var. *Sylvestris* proteome. The obtained olive protein sequences were searched against *Olea europaea* var. *Sylvestris* transcriptome. To find olive *SMT* gene sequences obtained transcript sequences were searched against *Olea europaea* var. *Sylvestris* genome. The *SMT* gene sequences were aligned with *SMT* transcript sequences to obtain exon regions. The following criteria were considered during primer designing: Tm value was optimum 60 ℃, and Tm difference between primers was at most 1°C. Furthermore, it was provided that at least one of the primer pairs binds to the junction of two exons so binding of primers to the genomic region of the same gene is prevented. According to the specified parameters, if an appropriate primer binding site cannot be found in the exon junctions, the primers were chosen to bind to different exons. It was provided that there must be an intron region consisting of at least 1000 base pairs between two exons. In case of any gene consisting of only one exon region (for example, *OeSMT2*) primers were selected within the coding regions in the transcripts of the genes of interest.

3.8. Determination of primer efficiencies

The amplification efficiency of designed SMT primers was determined by standard curve experiments. For this purpose cDNA was synthesized with Ayvalık RNA samples. 10-fold serial dilution of synthesized cDNAs was performed 6 times (Table 10). The 10-fold sequential dilutions of cDNAs were used as a template for SYBR Green-based qPCR reactions. For each primer pair, 10 µL qPCR reactions was prepared with SYBR® Green PCR Master Mix (Applied Biosystems, USA), 200nM forward and reverse primer, 1µl of cDNA (Table 11) and Step One Plus Real Time PCR System (Applied Biosystems, USA) was used for amplification of primers.

Table 10

1:10 serial dilution of cDNAs

Label of tube	Sample	Volume of sample	Volume of nuclease-free H_2O
1	Stock cDNA	15 µl	45 µl
2	1/10	6 µl (from tube 1)	54 µl
3	1/100	6 µl (from tube 2)	54 µl
4	1/1,000	6 µl (from tube 3)	54 µl
5	1/10,000	6 µl (from tube 4)	54 µl
6	1/10,0000	6 µl (from tube 5)	54 µl

Afterwards, a scatter plot was plotted with the log value of each sample dilution against obtained Ct values. The R^2 value and slope of the graph were calculated. The efficiency of primers was calculated by using the formula (3.1) (Dorak, 2007).

$$\text{Efficiency} = [10(-1/\text{slope})] - 1 \quad (3.1)$$

3.9. Gene expression analysis

Step One Plus Real Time PCR System (Applied Biosystems, USA) was used to analyse the relative gene expression levels of *SMT* genes. qPCR reactions were prepared as 10 µL for per well and contained SYBR® Green PCR Master Mix (Applied Biosystems, USA) (Table 11).

Table 11

Components of Real-time PCR reactions

Components	Volume	Final concentrations
SYBR® Green PCR Master Mix	5 µl	1x
Forward Primer	0,3 µl	0,05 µM
Reverse Primer	0,3 µl	0,05 µM
Template cDNA	1 µl	-
Nuclease-free H_2O	0,4 µl	-

Gene expression studies were completed with fruit tissue samples harvested at 8 different ripening stages from 4 olive cultivars (Ayvalık, Gemlik, Gökçeada, Memecik). Three biological replicates, each having three technical replicates were used for each sample (Figure 6). Endogenous control was provided by two reference genes (*CLATHRIN* and *pKABAI*) which have been identified by previous study (Hürkan et al., 2018).

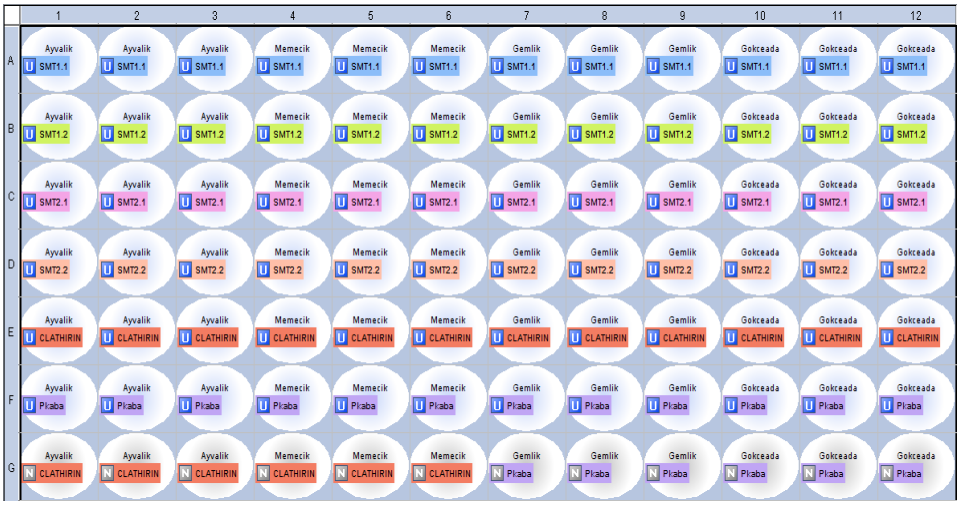

Figure 6. qPCR plate layout

The thermal cycling conditions included an initial denaturation step of 95 ºC for 10 min, followed by 40 cycles of 95°C for 15 s, 60°C for 60 s, and as an extension step of 72◦C for 1 min (Figure 7). At the end of the reaction, Melt Curve Analysis was performed between 60-95°C to obtain any the presence of non-specific products or primer dimers. Gene expression data were analysed by using comparative Ct (ΔCT) method (Pfaffl, 2001).

The error bars were determined by calculating the means ±SD of relative gene expression of three biological and three technical replicates for each sample. Statistical analysis of relative gene expression of *SMT* genes was run out by TUKEY test following the One-Way ANOVA with a 0.05 significance level for all statistical tests.

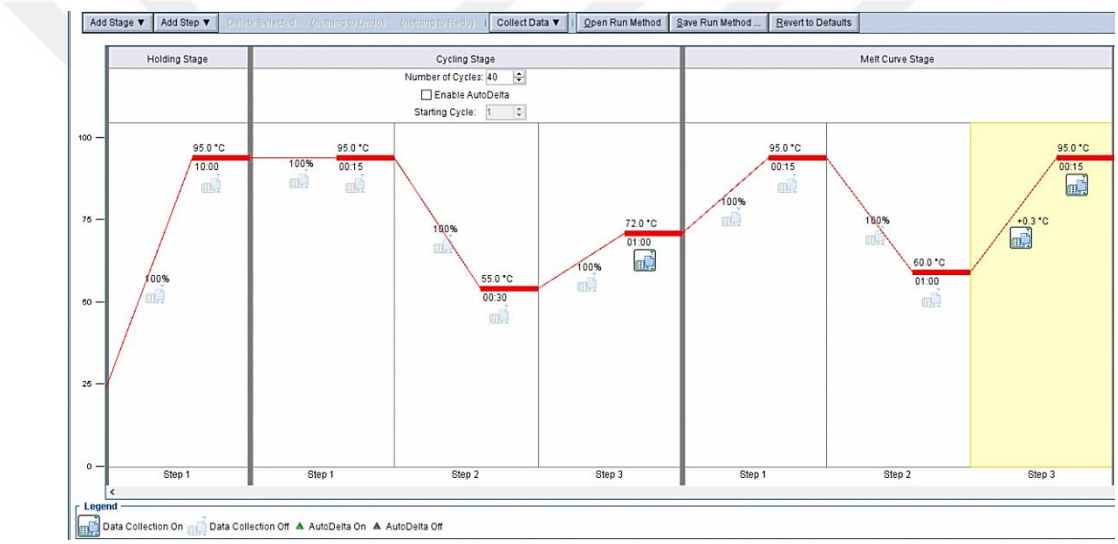

Figure 7. Thermal cycle of real-time PCR reactions.

CHAPTER 4
RESULTS AND DISCUSSION

4.1. Plant materials

For this study, three olive cultivars (Ayvalık, Memecik, and Gemlik) were chosen because of their high yield of oil (25% for Ayvalık, 24% for Memecik, 30% for Gemlik). These cultivars are the most cultivated varieties in the western coastal regions of Türkiye (Efe et al., 2013). Exclusively, the Gökçeada cultivar from the island of Gökçeada was chosen based on its native and distinctive cultivation habitat. Additionally, Gökçeada cultivar has significantly high PS content in its oil (Gül & Şeker, 2006). Olive fruit tissues were supplied at 15-day intervals for 8 ripening stages (Figure 8). Fruit samples of the cultivars were instantly frozen with liquid nitrogen after harvest and stored at -80 ºC until RNA isolation. The maturity index of olive fruits was calculated when they reached the laboratory. Fruit colour scales were determined based on the following indicators:

0 - Olives with dark green peel colour

1 - Olives with a yellow or yellowish-green peel

2 - Olives with a slightly reddish-yellow colour peel

3 - Olives with mostly reddish colour peel

4 - Olives whose peel colour is completely black and the pulp is still completely green or white

5 - Olives with a completely black peel colour and a magenta colour up to half of the flesh

6 - Olives whose peel colour is completely black and the part of the fruit flesh up to the core is magenta.

7 - Olives whose peel colour is completely black and fruit flesh and pit completely dark

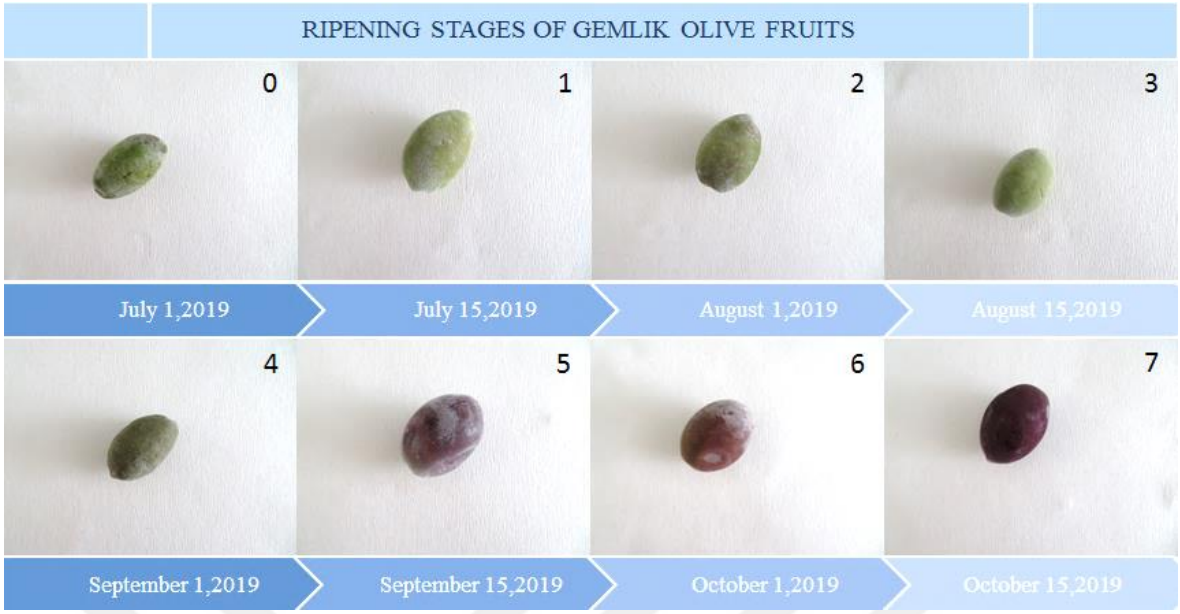

Figure 8. The olive fruit samples which were used for RNA isolation. The ripening stages of the fruits are indicated in the upper right corner of the image according to the colour scale used in the calculation of the maturity index.

4.2. RNA isolation and synthesis of cDNA

Following RNA isolation the quality and integrity of the RNAs were assessed with UV light after 1% agarose gel electrophoresis (Figure 9). The 28S and 18S rRNA bands were intact in the agarose gel electrophoresis. The Qubit assay was used to determine the quantities of RNA samples. The RNA concentrations of samples range from 176 to 1072 ng/µL (Table 12). In order to avoid DNA contamination, DNAse I treatment was carried out once RNA concentrations were measured. 1000 ng of RNA from each sample was used for cDNA synthesis.

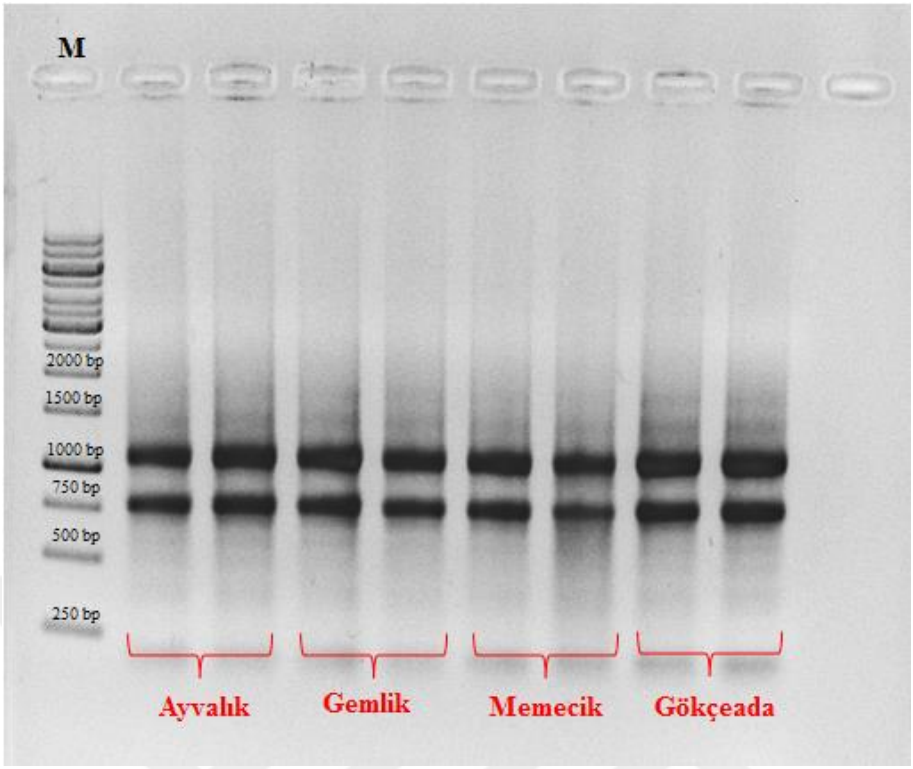

Figure 9. Gel image of July 1, 2019 RNA samples of olive fruit tissues. M: 1 kb DNA Ladder

Table 12

The RNA concentrations of olive oil samples for 8 ripening stages

RNA samples	Ayvalık (ng/µL)	Memecik (ng/µL)	Gemlik (ng/µL)	Gökçeada (ng/µL)
July 1, 2019	480	436	500	554
July 15, 2019	310	596	324	260
August 1, 2019	264	896	460	370
August 15, 2019	554	666	348	342
September 1, 2019	252	808	378	176
September 15, 2019	628	1072	668	352
October 1, 2019	438	618	406	240
October 15, 2019	262	586	282	350

4.3. Bioinformatic analysis

In this research, bioinformatic analysis was carried out to obtain *SMT* genes in the olive genome by using available databases. The genome, transcriptome, and proteome data of *Olea europaea* var. *Sylvestris* were downloaded from NCBI and added as a BLAST database into Geneious v.8.1 software. The identification of olive *SMT* genes in the Sylvestris genome was achieved with BLAST analysis. Reference *A. thaliana* protein sequences of *SMT1* (AT5G13710), *SMT2* (AT1G20330), and *SMT3* (AT1G76090) genes were obtained TAIR and BLASTp analysis was performed against the Sylvestris proteome by using the Geneious v.8.1 software. Among the protein sequences obtained according to the BLASTp result, the sequences with the E-value closest to 0 as well as the highest coverage and similarity percentage were determined.

Afterward, an UPGMA phylogenetic tree was plotted with candidate olive protein sequences, reference *A. thaliana* and *S. lycopersicum* protein sequences in Geneious v.8.1. As demonstrated in Figure 10, all SMT sequences clustered into two large branches. The *OeSMT1* sequences gathered in one branch, while *OeSMT2* and *OeSMT3* sequences gathered in another. Similar to the earlier studies *SMT* genes were classified into two different groups of genes also in olive (*OeSMT1* and *OeSMT2*) as distinct from *Arabidopsis*. The olive sequences shows clustered with reference SMT sequences with higher than 65% similarity were selected for use in further studies in this research.

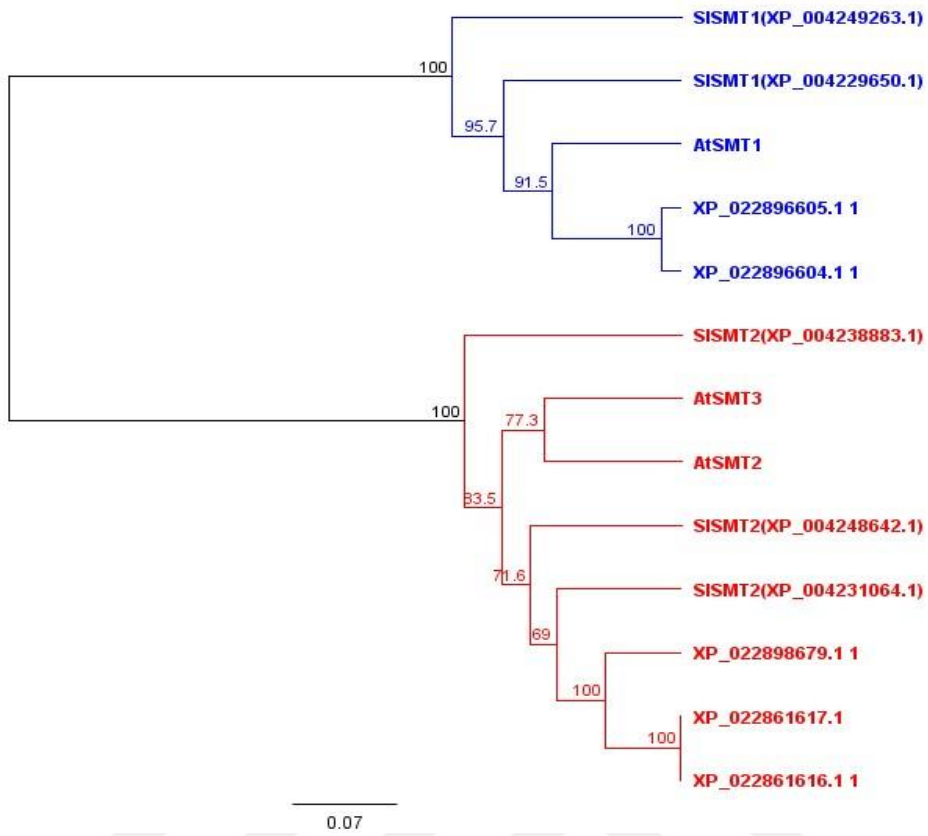

Figure 10. Phylogenetic tree for sterol methyltransferase protein sequences

Determined olive protein sequences were searched against Sylvestris transcriptome with the tBLATSn program. 9 candidate olive SMT transcripts were selected according to E-value, coverage and similarity percentage (Figure 11). Three olive transcript sequences (XM_023040836,1, XR_002705702,1, and XM_023040837,1) were identified for *OeSMT1*, and it was observed that the identity of transcript sequences was higher than 77% and the length of sequences ranged from 1182 to 1315 bp. Likewise, three olive transcript sequences (XM_023005848,1, XM_023005849,1, and XM_023042911,1) were identified for *OeSMT2*, and it was observed that the identity of transcript sequences was higher than 73% and the length of sequences ranged from 1518 to 1529 bp. The transcript sequences of *OeSMT3* were found similar with *OeSMT2*, however the identity was obtained higher than 71%.

Name	Description	% Identical Sites	E Value	Sequence Length
XM_023005848.1	PREDICTED: Olea europaea var. sylvestris 24-methylenesterol C-methyltransferase 2-like (LOC111381992),...	73.1%	0	1,518
XM_023005848.1	PREDICTED: Olea europaea var. sylvestris 24-methylenesterol C-methyltransferase 2-like (LOC111381992),...	71.9%	3.63e-152	1,518
XM_023005849.1	PREDICTED: Olea europaea var. sylvestris 24-methylenesterol C-methyltransferase 2-like (LOC111381993),...	73.1%	0	1,521
XM_023005849.1	PREDICTED: Olea europaea var. sylvestris 24-methylenesterol C-methyltransferase 2-like (LOC111381993),...	71.9%	3.63e-152	1,521
XM_023042911.1	PREDICTED: Olea europaea var. sylvestris 24-methylenesterol C-methyltransferase 2-like (LOC111412135),...	73.6%	0	1,529
XM_023042911.1	PREDICTED: Olea europaea var. sylvestris 24-methylenesterol C-methyltransferase 2-like (LOC111412135),...	71.3%	9.75e-147	1,529
XM_023009755.1	PREDICTED: Olea europaea var. sylvestris cycloartenol-C-24-methyltransferase-like (LOC111385373), mRNA	73.0%	3.69e-64	595
XM_023040836.1	PREDICTED: Olea europaea var. sylvestris cycloartenol-C-24-methyltransferase-like (LOC111410481), trans...	78.0%	0	1,315
XR_002705702.1	PREDICTED: Olea europaea var. sylvestris cycloartenol-C-24-methyltransferase-like (LOC111410481), trans...	78.0%	0	1,315
XM_023040837.1	PREDICTED: Olea europaea var. sylvestris cycloartenol-C-24-methyltransferase-like (LOC111410482), mRNA	77.2%	0	1,182

Figure 11. The candidate transcript sequences of the olive *SMTs*

Consequently, the candidate transcript sequences were searched against the Sylvestris genome with the BLASTn program to detect *OeSMT* gene regions. 2 homoeologous *OeSMT1* genes were found in Sylvestris genome and these genes are located on chromosome 15 and were named as *OeSMT1* (LOC1111410481), and *OeSMT1.2* (LOC1111410482) respectively. Exon regions were extracted from the detected gene regions and *OeSMT* coding sequences (CDS) were obtained. Based on the bioinformatics analysis, it was detected that the CDS of the *AtSMT1* gene is composed of 1011 bp and contains 13 exon regions. Whereas the CDS of the *OeSMT1* and *OeSMT1.2* genes is composed of 987 bp, and 981 bp. Both of them contain 12 exon regions and a high degree of identity (98%) was observed between them.

2 homoeologous *OeSMT2* genes were found in Sylvestris genome and these genes are located on chromosome 16 were named as *OeSMT2* (LOC111381993), and *OeSMT2.1* (LOC1111412135) respectively. The CDS of the *AtSMT2* gene is composed of 1086 bp while the CDS of the *OeSMT2* and *OeSMT2.1* genes in the olive genome include 1083 bp and 1092 bp. Also, both of them are composed of only one exon region and a high degree of identity (79%) was observed between them. Finally, appropriate primers were designed according to these CDS for forthcoming gene expression studies (Figure 12).

Name	Description	First Residues	Sequence Length	Tm	%GC	Hairpin	Primer-Dimer
SMT2 R	Single Exon Gene	CTTTGGGACGGCGGAAAAAG	20	60	55.0%	-	10.6
SMT2 F	Single Exon Gene	TTCAACTCTCTGGCGGTTCC	20	60	55.0%	-	-
SMT2.1 R	Single Exon Gene	TGCGATTTTCCAGGAACGGA	20	60	50.0%	-	11.5
SMT2.1 F	Single Exon Gene	GTCGTTTTTCCGGAGACCCA	20	60.3	55.0%	-	3
SMT1.2_R	SMT1.2 spesific Exon-junction	TGGAGATACTGAAAAGGCGAGA	22	58.9	45.5%	-	-
SMT1.2_F	SMT1.2 spesific Exon-junction	AGGCCTCAGCTCTCTACACT	20	59.7	55.0%	39.7	1.4
SMT1_R	Binds to both Exon-junction	TAGCACCCAACAGCATCTGG	20	60	55.0%	35.5	-
SMT1_F	Binds to both Exon-junction	AGGAAAGGCCCTAAACCGTG	20	60	55.0%	37.4	-

Figure 12. Information on designed primers for *OeSMT* genes

4.4. Cloning and Comparative analysis of *OeSMT* genes

In this study for the comparative analysis of *OeSMT* genes, required cloning primers were designed and *OeSMT* (*OeSMT1, OeSMT2.1,* and *OeSMT2.2*) genes were cloned successfully. In order to produce the amplicons required for the cloning of *OeSMT* genes, polymerase chain reactions were set up to examine different temperatures using chosen primers. Three distinct temperatures (54 °C, 57 °C, and 60 °C) were tried to detect the optimal primer binding temperature. Obtained PCR products were assessed with 1% agarose gel electrophoresis under UV light and desired bands which representing the amplicon size of *OeSMT1, OeSMT2.1,* and *OeSMT2.2* (respectively 702, 954, and 1266 bp) were observed (Figure 13 and 14).

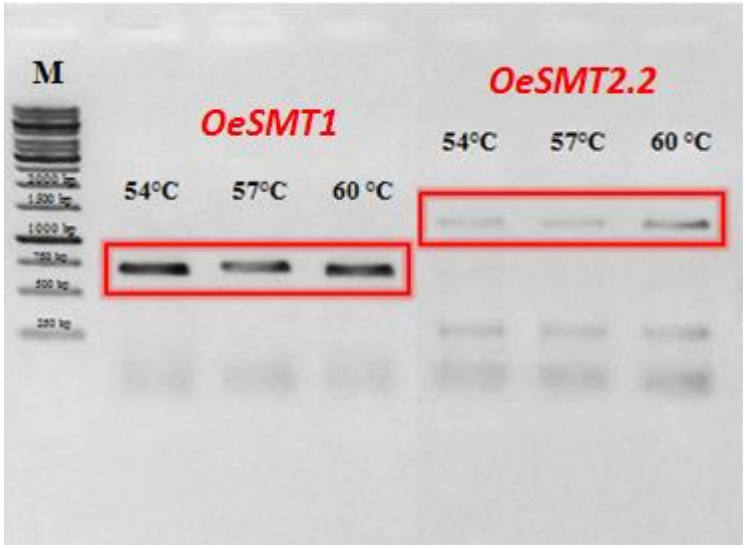

Figure 13. The products of *OeSMT1* and *OeSMT2.2* after gradient PCR. M: 1 kb DNA Ladder

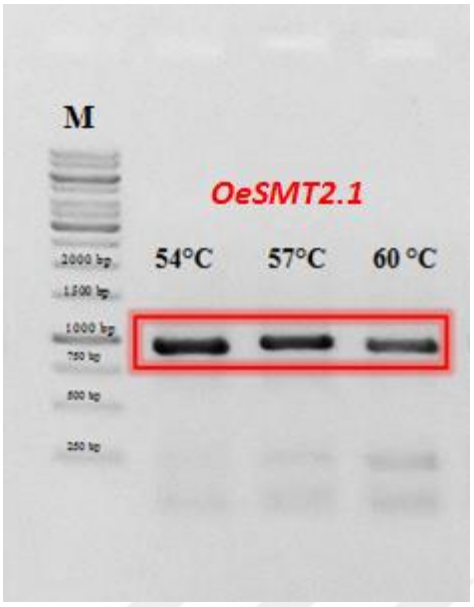

Figure 14. The products of *OeSMT2.1* after gradient PCR. M: 1 kb DNA Ladder

Following gradient PCR, the correct *OeSMT* amplicons were sliced from agarose gel by using a sterile surgical blade and extracted from gel slices by using a gel extraction kit and extracted *OeSMT* amplicons were visualized again on agarose gel with a UV light transilluminator for validation (Figure 15).

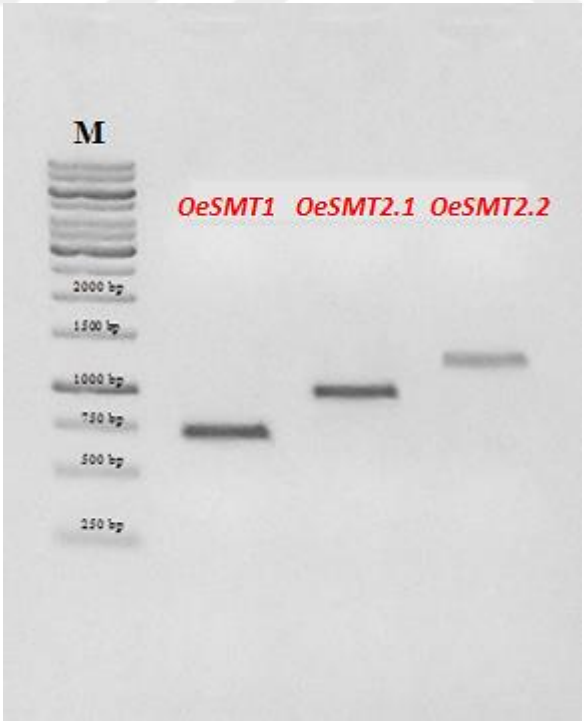

Figure 15. Reimaged *OeSMT1, OeSMT2.1,* and *OeSMT2.2* products after gel extraction. M: 1 kb DNA Ladder

Subsequently, the extracted *OeSMT* amplicons were ligated with the pCR™-Blunt vector for transformation. The *E. coli* DH10B strain was simultaneously prepared for transformation by giving them a component property. Then recombinant vectors were transformed into component bacteria with the heat shock method. Transformed *E. coli* cells were incubated in a selective LB media for overnight. The following day, bacteria colony growth was observed (Figure 16), and some of them were picked as templates for colony PCR.

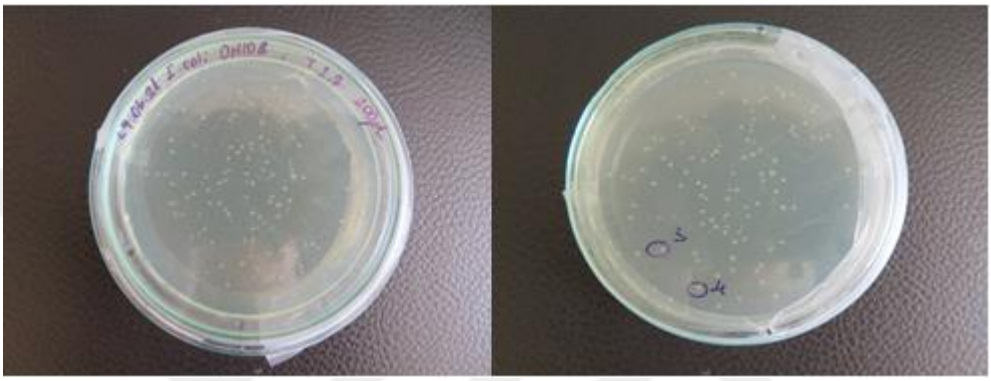

Figure 16. *E. coli* colonies incubated overnight in selective medium

To validate that *OeSMTs*::pCR™-Blunt recombinant vector has successfully inserted in *E. coli* cells, colony PCR products were assessed with 1% agarose gel electrophoresis (Figure 17 and 18). After colony PCR, positive colonies confirmed to harbour *OeSMT* genes were inoculated in sterile LB broth containing Kanamycin and incubated overnight at 37 °C in a shaking incubator.

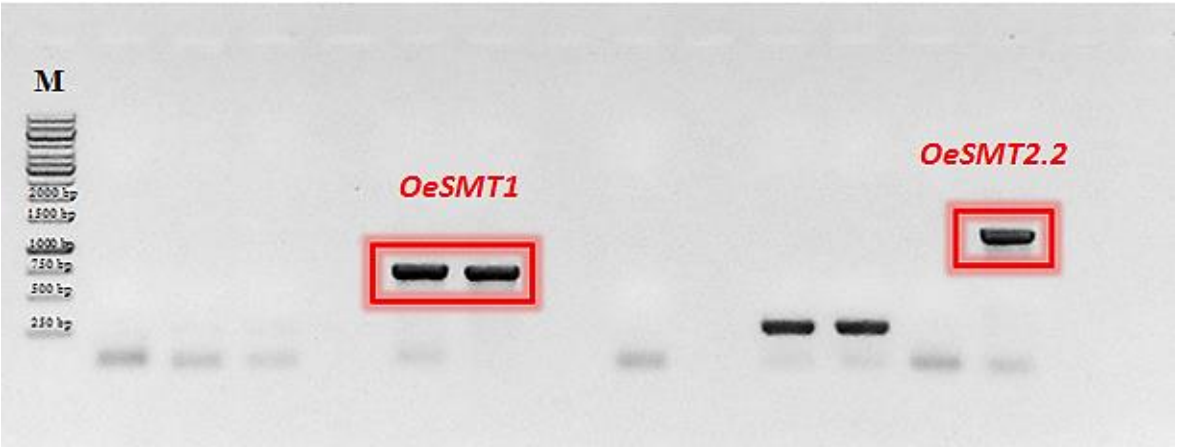

Figure 17. Colony PCR results of *OeSMT1* and *OeSMT2.2* M: 1 kb DNA Ladder

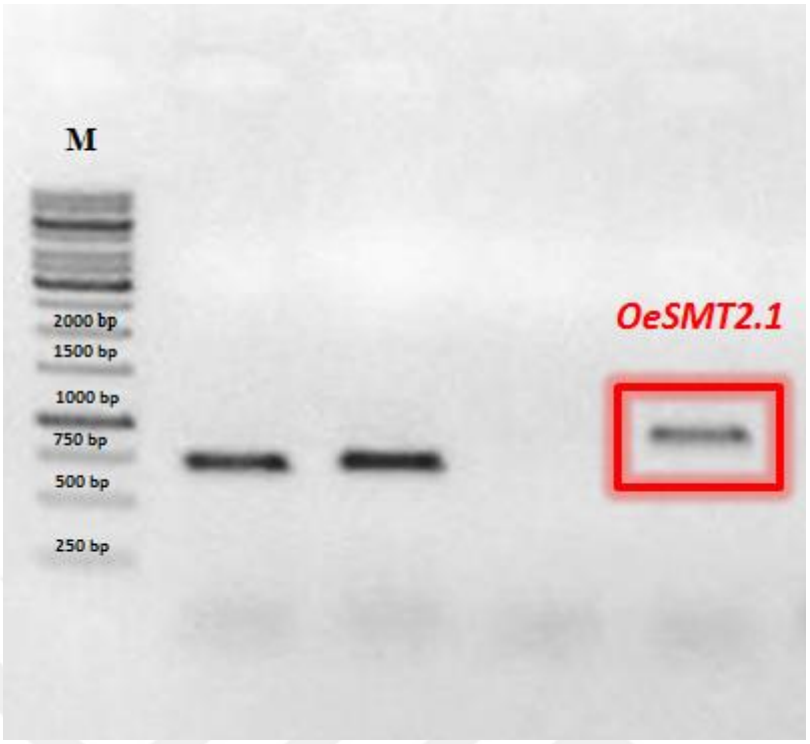

Figure 18. Colony PCR results of *OeSMT2.1* M: 1 kb DNA Ladder

The next day, plasmids were isolated from the recombinant *E. coli* cells which were incubated in selective LB media for a night. The digestion of *OeSMT* amplicons from isolated recombinant plasmids were provided by using FastDigest EcoRI (FD0274, Thermo Scientific™) and FastDigest XhoI (FD0694, Thermo Scientific™) enzymes. The product size of the digested plasmids was visualized with a UV transilluminator system after 1% agarose gel electrophoresis (Figure 19 and 20). FastDigest EcoRI digests the plasmid in two regions whereas FastDigest XhoI digests the plasmid in only one region. When the recombinant plasmids of *OeSMT1* and *OeSMT2.1* were digested with FastDigest EcoRI enzyme, the bands of *OeSMT* amplicons were observed at the bottom of the gel, and the 3500 bp bands of pCR™-Blunt vector were observed at the top of the gel (Figure 19).

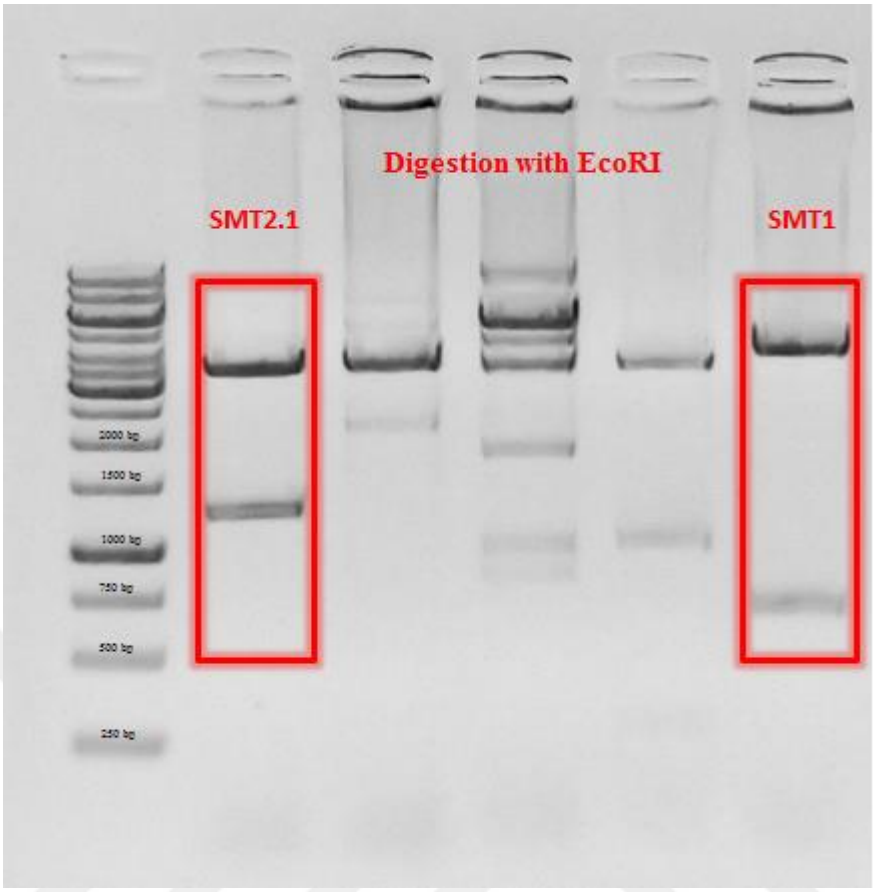

Figure 19. Plasmid digestion with double-cut EcoRI

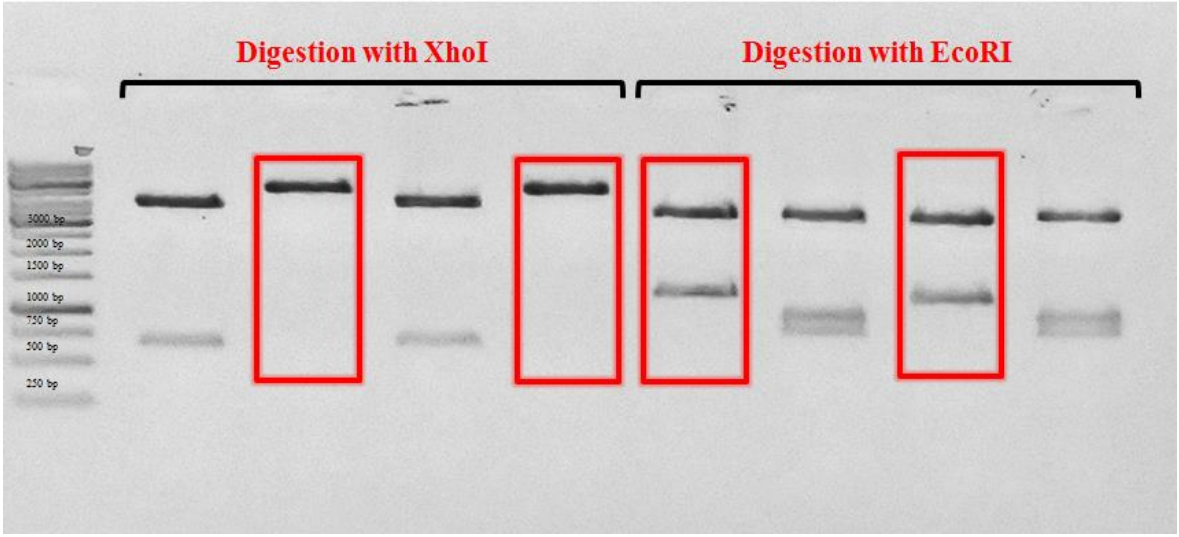

Figure 20. Plasmids digestion of *OeSMT2.2*::pCR™-Blunt vector with single-cut XhoI and double-cut EcoRI enzymes

4.5. Sequence alignment and phylogenetic analysis of *OeSMTs*

In this part of the study, the sequences of successfully cloned *OeSMT* genes were determined. The deduced consensus sequence of *OeSMT1* was composed of 583 bp (Figure 21). This consensus sequence was searched by BLASTn against other plant species in the NCBI database. The highest identity of *OeSMT1* was observed consecutively in *Erythranthe guttatus* species with 83,01% and 7e-164 of E-value, *Camellia sinensis* species with 82,11% and 9e-163 of E-value, and *Helianthus annuus* species with 83,03% and 1e-160 of E-value (Figure 3 Suppl.).

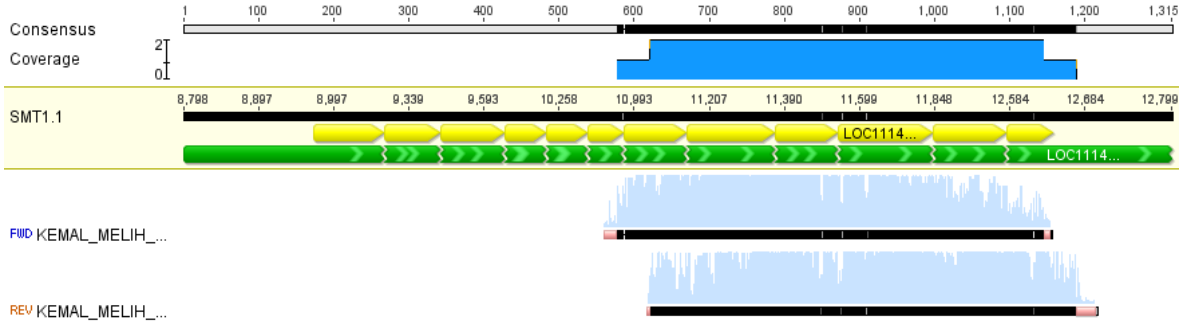

Figure 21. *OeSMT1* consensus sequences and assembled chromatogram sequences

The deduced consensus sequence of *OeSMT2.1* gene composed of 897 bp (Figure 22). This consensus sequence of *OeSMT2.1* was searched by BLASTn against other plant species in the NCBI. The highest identity of *OeSMT2.1* was observed consecutively in *Sesamum indicum* species with 81,92% and 0 of E-value, *Nicotiana attenuata* species with 78,87% and 0 of E-value, and *Capsicum annuum* species with 78,87% and 0 of E-value (Figure 4 Suppl.).

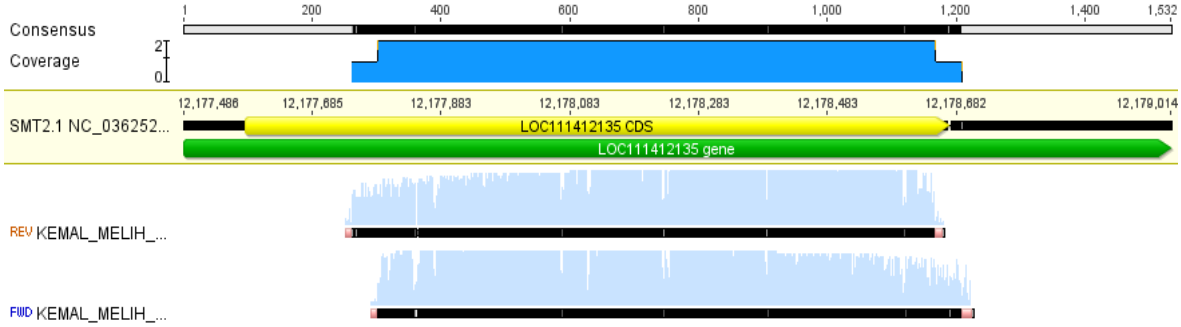

Figure 22. *OeSMT2.1* consensus sequences and assembled chromatogram sequences

The deduced consensus sequence of *OeSMT2.2* gene composed of 1088 bp (Figure 23). This consensus sequence of *OeSMT2.2* was searched by BLASTn against other plant species in the NCBI. The highest identity of *OeSMT2.2* was observed consecutively in *Sesamum indicum* species with 79,80% and 0 of E-value, *Ipomoea triloba* species with 76,92% and 0 of E-value, and *Nicotiana tomentosiformis* species with 76,98% and 0 of E-value (Figure 5 Suppl.)

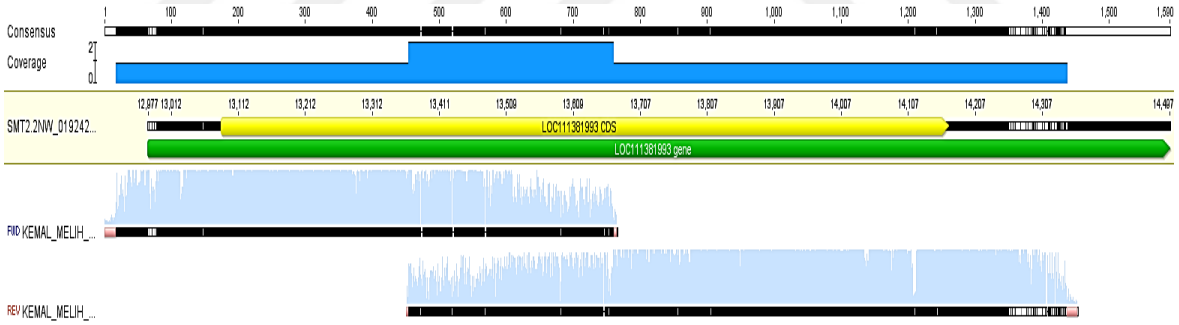

Figure 23. *OeSMT2.2* consensus sequences and assembled chromatogram sequences

The deduced amino acid sequences of *OeSMT* genes were aligned with the SMT protein sequences of *A. thaliana* and the similarity of these sequences was investigated. Protein sequence of OeSMT1 was exhibit the 82.7% similarity with the AtSMT1 while OeSMT2 protein sequences were 79% (OeSMT2.1) and 81.3% (OeSMT2.2) similar with the AtSMT2.

The binding sites for sterols and AdoMet are required to be found in the SMT proteins (Nes et al., 2003). Therefore, conserved amino acid regions were searched in the deduced OeSMT sequences with the NCBI Conserved Domain Search program, and three sterol binding sites and AdoMet binding site were revealed (Figure 24).

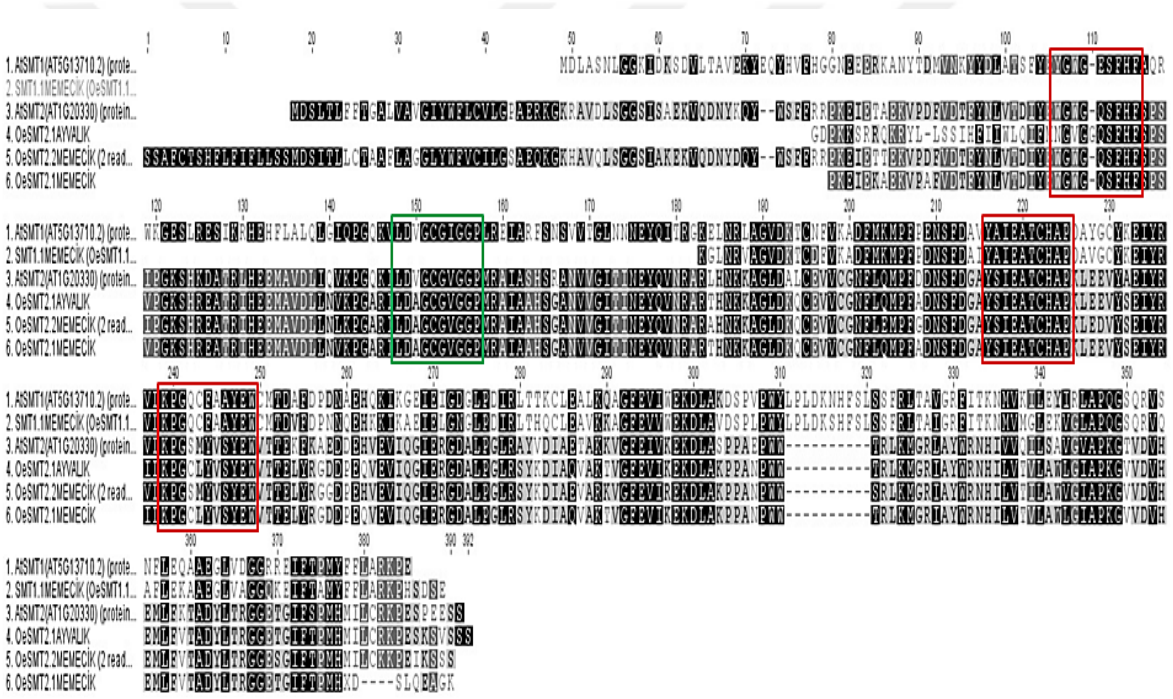

Figure 24. Sequence alignment of OeSMT proteins with reference AtSMT protein sequences. Conserved motifs for sterol binding sites were represented by red rectangles and for AdoMet binding site was represented by a green rectangle.

The homology of deduced olive *SMT* genes were searched against the SMT sequences of other plant species by using BLASTn program. A phylogenetic tree was constructed based on the results of the BLASTn analysis (Figure 25). Also, the sequences of Farga and Arbequina cultivars were included in this tree. When we interpreted this phylogenetic tree, it was observed that the *OeSMT1.1*, *OeSMT2.1*, and *OeSMT2.2* genes were each grouped in a separate branch of the tree.

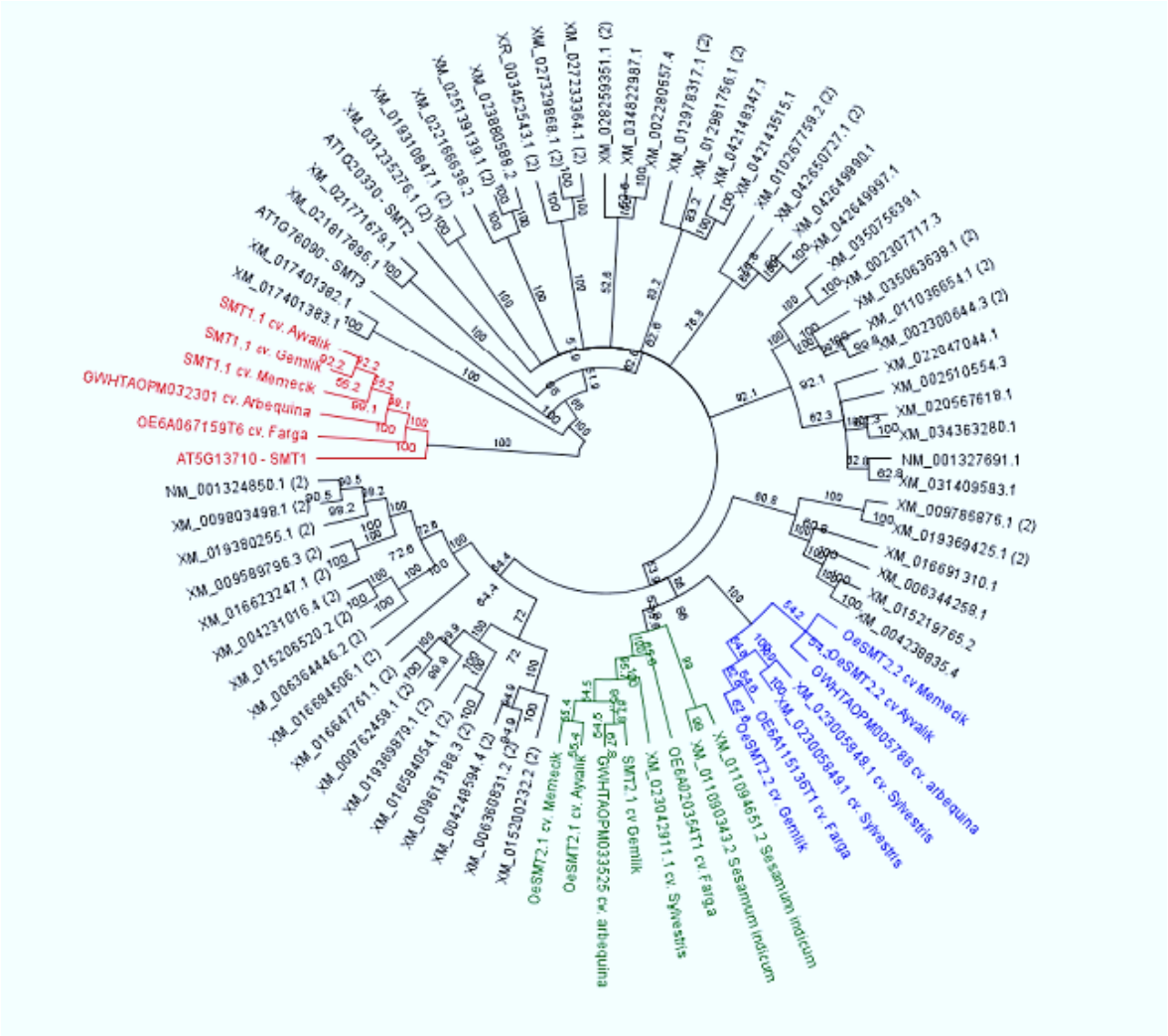

Figure 25. Phylogenetic tree for *SMT* transcripts

4.6. Gene expression studies

4.6.1. The efficiency of primers

By employing 10-fold serial dilutions of cDNA templates of *SMTs*, the standard curve analysis was used to determine primer efficiency. For this purpose, real-time PCR reactions were established using serial dilutions of cDNAs obtained from *SMT* amplifications. Based on the standard curve analysis, only primer pairs with efficiency values in the range of 90–110% and R^2 values greater than 0.98 were used during gene expression studies (Table 13).

Table 13

Information on primers used in gene expression studies

Primer name	Gene accession code	Primer sequence	Efficiency (%)	R^2 value
SMT1_F	XM_023040836.1	AGGAAAGGCCCTAAACCGTG	99,1	0,9993
SMT1_R	XM_023040837.1	TAGCACCCAACAGCATCTGG		
SMT1.2_F	XM_023040837.1	AGGCCTCAGCTCTCTACACT	100,4	0,9976
SMT1.2_R		TGGAGATACTGAAAAGGCGAGA		
SMT2_F	XM_023005849.1	TTCAACTCTCTGGCGGTTCC	99,7	0,9998
SMT2_R	XM_023042911.1	CTTTGGGACGGCGGAAAAAG		
SMT2.1_F	XM_023042911.1	GTCGTTTTTCCGGAGACCCA	90,0	0,9983
SMT2.1_R		TGCGATTTTCCAGGAACGGA		

Primer efficiency of SMT1_F and SMT1_R pairs was determined via standard curve analysis (Figure 26). The primer efficiency graph was plotted with the Ct values obtained by quantitative PCR. The R^2 value was obtained as 0.9993 while the efficiency of the reaction was obtained as 99.1%. The curve was found to be sufficiently linear hence the relevant primer pair was decided to be appropriate for gene expression experiments.

Dilutions	Sample quantity	Log	ct values	Dilution Rate =	10
1.	1000000	6	21,013308		
2.	100000	5	24,54242		
3.	10000	4	28,061808	Target =	SMT1
4.	1000	3	31,103974	Templete =	Olive fruit cDNA
5.	100	2	34,449627	Slope =	-3,34341925
6.	10	1		Efficiency (%) =	**99,1**

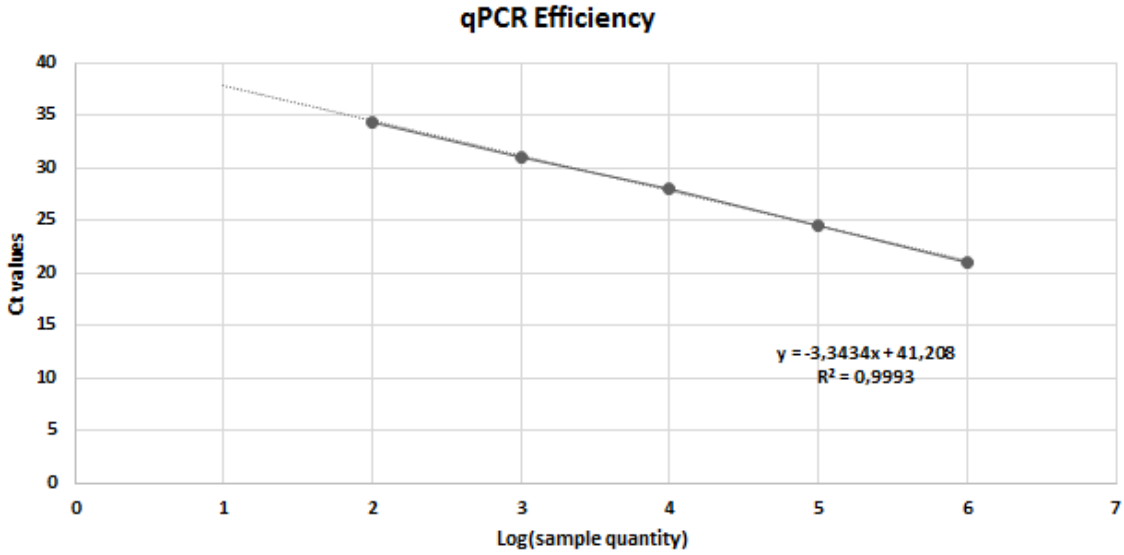

Figure 26. The efficiency curve of SMT1 primer pair

Primer efficiency of SMT1.2_F and SMT1.2_R pairs was determined standard curve analysis (Figure 27). The primer efficiency graph was plotted with the Ct values obtained by quantitative PCR. The R^2 value was obtained as 0.9976 while the efficiency of the reaction was obtained as 110.4 %. The curve was found to be sufficiently linear hence the relevant primer pair was decided to be appropriate for gene expression experiments.

Dilutions	Sample quantity	Log	ct values	Dilution Rate =	10
1.	1000000	6	26,865835		
2.	100000	5	29,708025		
3.	10000	4	33,424924	Target =	SMT1.2
4.	1000	3	36,666231	Templete =	Olive fruit cDNA
5.	100	2		Slope =	-3,31180851
6.	10	1		Efficiency (%) =	**100,4**

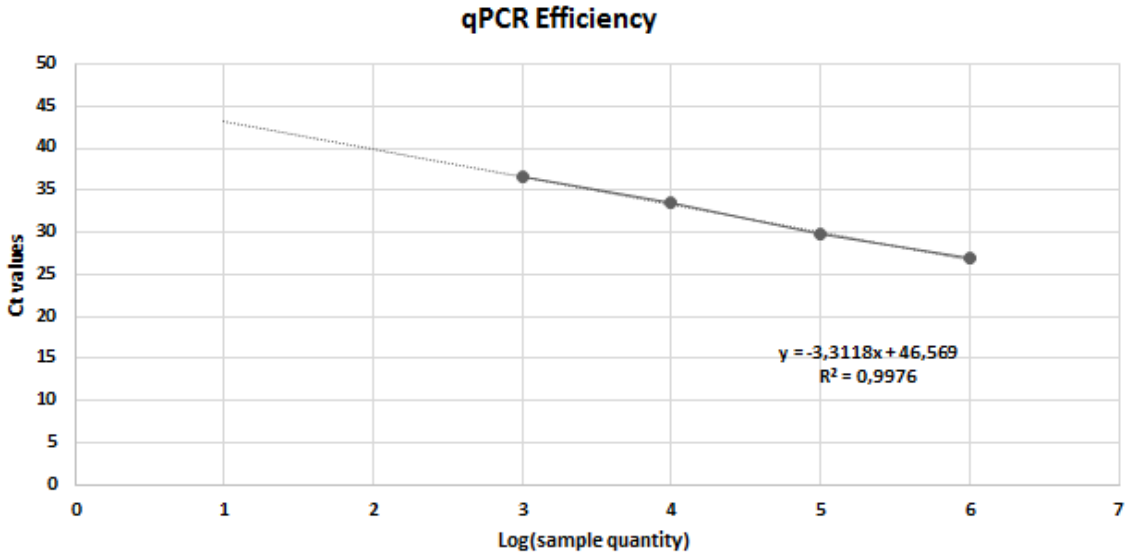

Figure 27. The efficiency curve of SMT1.2 primer pair

Primer efficiency of SMT2_F and SMT2_R pairs was determined standard curve analysis (Figure 28). The primer efficiency graph was plotted with the Ct values obtained by quantitative PCR. The R^2 value was obtained as 0.9998 while the efficiency of the reaction was obtained as 99.7 %. The curve was found to be sufficiently linear hence the relevant primer pair was decided to be appropriate for gene expression experiments.

Dilutions	Sample quantity	Log	ct values	Dilution Rate =	10
1.	1000000	6	21,859137		
2.	100000	5	25,275635		
3.	10000	4	28,674163	Target =	SMT2
4.	1000	3	31,828793	Templete =	Olive fruit cDNA
5.	100	2	35,232714	Slope =	-3,33003114
6.	10	1		Efficiency (%) =	99,7

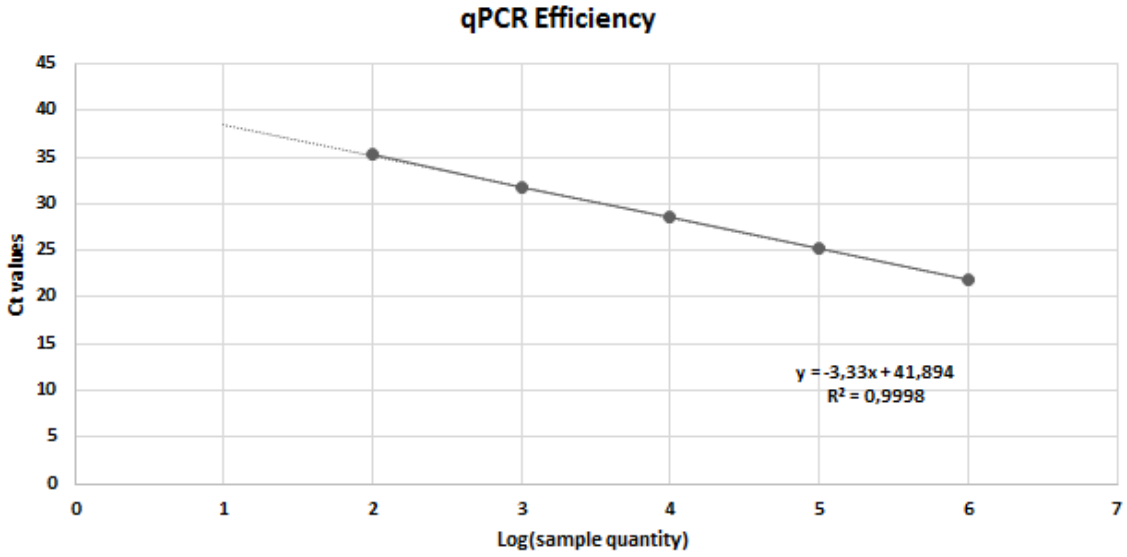

Figure 28. The efficiency curve of SMT2 primer pair

Primer efficiency of SMT2.1_F and SMT2.1_R pairs was determined standard curve analysis (Figure 29). The primer efficiency graph was plotted with the Ct values obtained by quantitative PCR. The R^2 value was obtained as 0.9983 while the efficiency of the reaction was obtained as 90 %. The curve was found to be sufficiently linear hence the relevant primer pair was decided to be appropriate for gene expression experiments.

Dilutions	Sample quantity	Log	ct values	Dilution Rate =	10
1.	1000000	6	26,216765		
2.	100000	5	29,36248		
3.	10000	4	33,193035	Target =	SMT2.1
4.	1000	3	36,896841	Templete =	Olive fruit cDNA
5.	100	2		Slope =	-3,58707844
6.	10	1		Efficiency (%) =	**90,0**

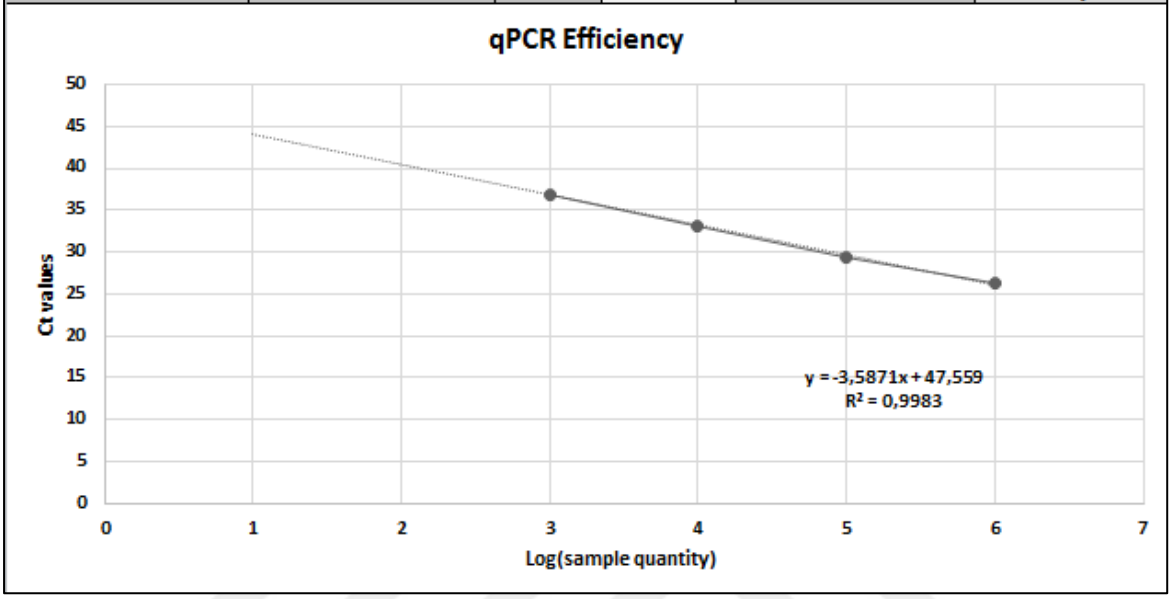

Figure 29. The efficiency curve of SMT2.1 primer pair

Melt Curve Analysis was performed as the final step of qPCR reactions between temperatures of 60-95°C. When the graphs were examined, no multi-peak rise was observed in the melting curve, proving that there were no contaminating or off-target amplification products (Figure 30).

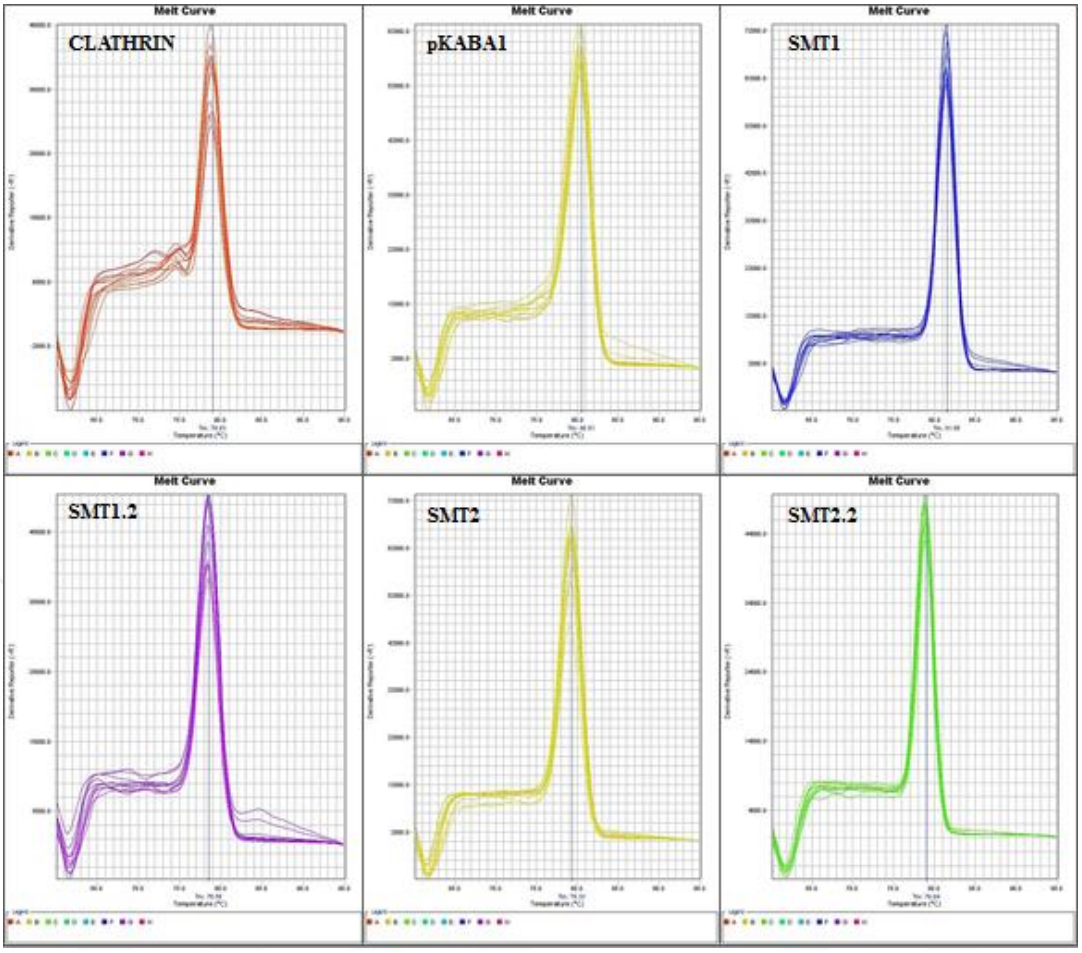

Figure 30. Melt curve analysis of *OeSMT* genes and housekeeping genes

4.6.2. The expression studies of *OeSMT* genes in olive fruit tissue

SMT genes, which play a key role in PS biosynthesis, are of great importance as they determine the final PS content and, relatedly, are effective in many biological processes (Schrick et al., 2004). In this part of the study, the expression levels *OeSMT* genes in four olive cultivars were determined by quantitative Real-Time PCR. Throughout eight consecutive ripening periods, cDNA was synthesized using RNAs extracted from olive fruits and used in Real-Time PCR reactions. Gene expression results were analysed with the comparative Ct (ΔCt) method and a relative gene expression graph was drawn for each *OeSMT* gene by using Ayvalık samples harvested on July 1, as a control group. *SMT1* are responsible for the C24 methylation of cycloartenol and thus the adjustment of the balance between cholesterol and alkylated sterols in the higher plants.

In the previous studies poor reproduction, an inconsistent vascular system, and abnormalities in auxin transport were observed in *Arabidopsis smt1*,*smt1/cph*, and *smt1*^{orc} mutants (Diener et al., 2000; Willemsen et al., 2003). Hence, the expression of *SMT1* has a great influence in determining the final PS ratio and, accordingly, in maintaining various biological processes (Schaeffer et al., 2001).

When the *OeSMT1* gene expression results were evaluated, it was observed that *OeSMT1* expression reached the highest level in all cultivars with the exception of Memecik on August 1 (Figure 31). The increase could be claimed to be sensible if considering the *SMT1* genes have a role at the beginning of the PS biosynthesis. Moreover, parallel with the up-regulation of *OeSMT1* an increase in PS content in olive cultivars was observed on this date (Figure 2 Suppl.). Consequently, this period can be regarded as the period when the synthesis rate of PSs increased. A dramatic decrease in *OeSMT1* expression was observed in all cultivars on September 15, followed by an increase in *OeSMT1* gene expression on October 1. When all cultivars were examined individually, it was noticed that Ayvalık, Gemlik, and Gökçeada all showed a consistent pattern of *OeSMT1* gene expression. However, when the results are considered comparatively, it is remarkable that the expression of this gene is higher in Gökçeada than in other cultivars.

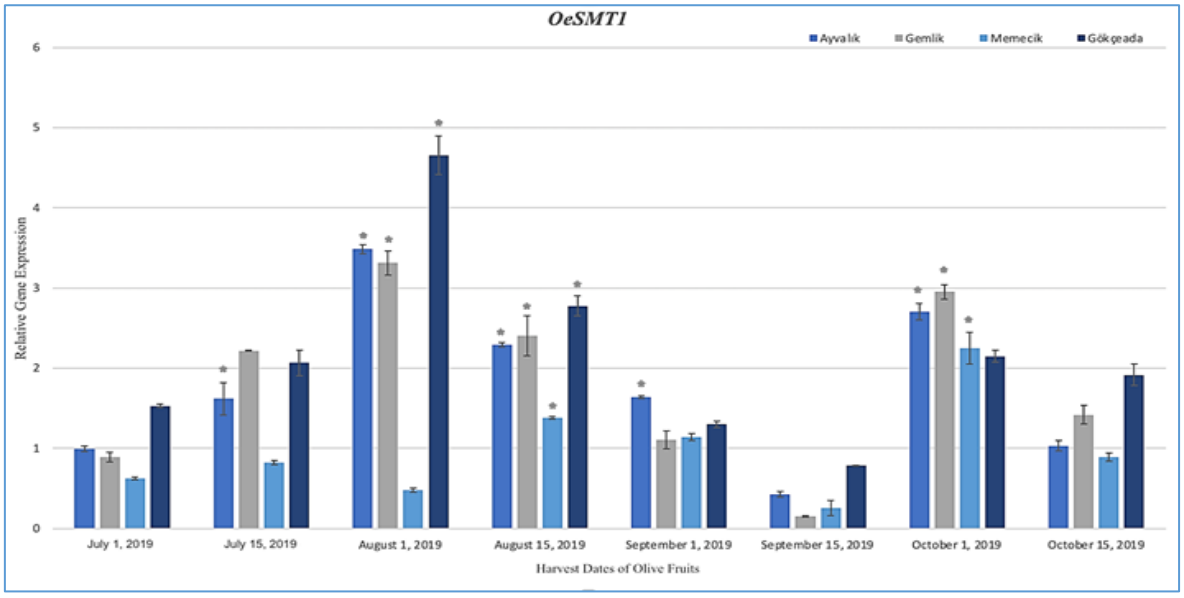

Figure 31. Gene expression results of the *OeSMT1* (Error bars represent standard error and asterisks represent statistically significant differences at P <0.05 based on Tukey's test).

When the *OeSMT1.2* gene expression results were evaluated, it was observed that *OeSMT1.2* expression was high in Ayvalık and Gemlik cultivars rather than the other cultivars (Figure 32). Notably, the highest expression of this gene belonged to Gemlik cultivar on July 15. Additionally, on October 15, all cultivars exhibited the lowest *OeSMT1.2* expression levels. Therefore, October 1 can be considered as the most convenient harvest date for these varieties.

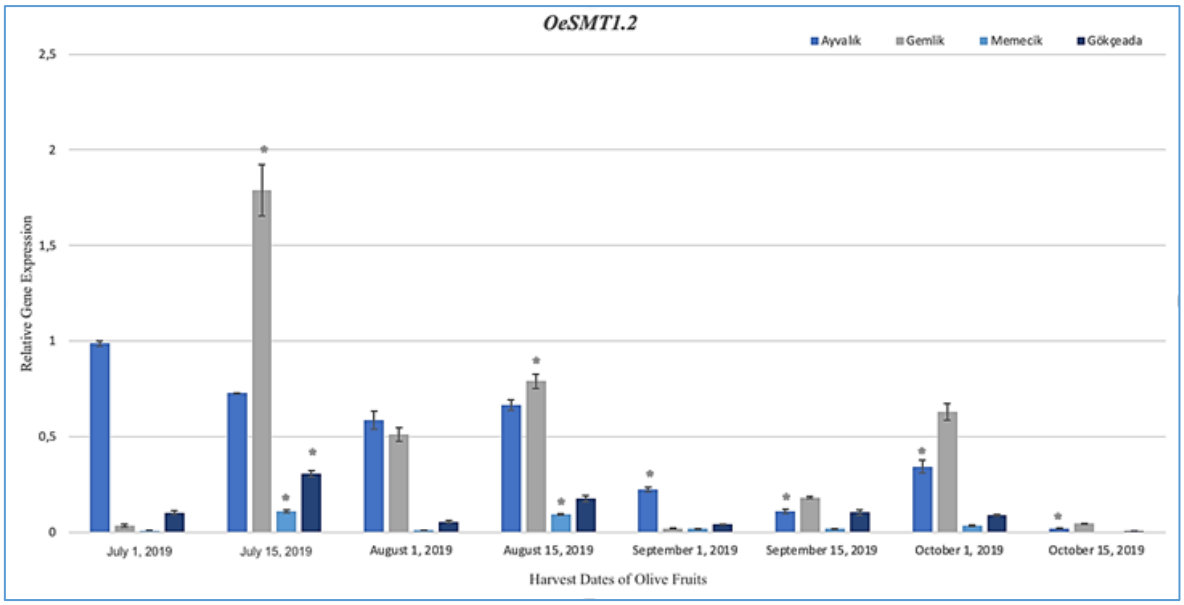

Figure 32. Gene expression results of the *OeSMT1.2* (Error bars represent standard error and asterisks represent statistically significant differences at P <0.05 based on Tukey's test).

The second methylation is provided by the other member of sterol transferases, *SMT2*, which is crucial for the balance in the final concentration between 24-methyl and 24-ethyl sterol. According to earlier research upon *smt2* mutants absence of *SMT2* gene expression cause alteration in the eventual ratio of β-sitosterol and campesterol and various morphological abnormalities in the plant morphology (F. Carland et al., 2010).

Considering gene expression studies of *OeSMT2*, this gene revealed the highest expression in all olive cultivars on August 15 (Figure 33). An increase in the PS content of the Picual and Arbequina oil was observed between September and November in a previous study (Fernández-Cuesta et al., 2013). Similarly, the higher level of *OeSMT2* expression in Sylvestris from August to October may have contributed to the elevated PS content of olives. On October 15, the lowest expression levels were observed in the Gökçeada cultivar, while the Ayvalık cultivar displayed the highest expression levels in this period compared to other cultivars. In general sight, the expression of the *OeSMT2* gene was observed continuously through all fruit ripening stages. In a previous study, expression of the *SMT2* gene was examined at the early fruit ripening stage, and an up-regulated gene expression was observed (Inês et al., 2019). Similarly in this study, an increase in *OeSMT2* gene expression was observed on August 15. Also the unexpected decrease in *Oe*SMT2 expression on August 1, might be proof the expression of this gene is affected by external conditions (Navas-López et al., 2020).

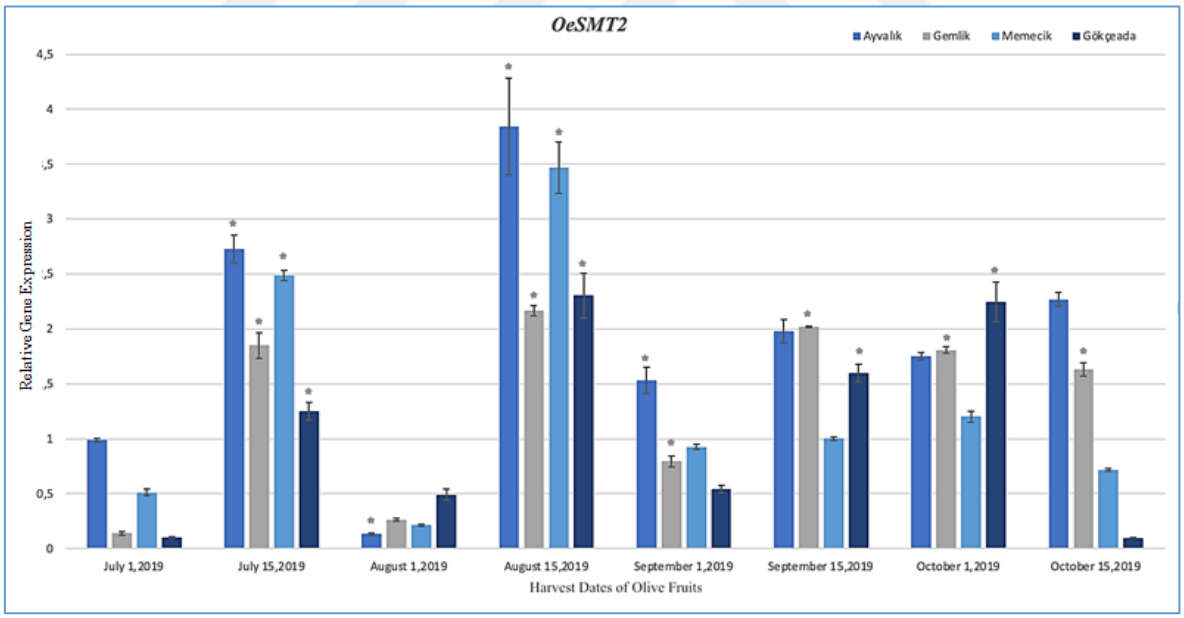

Figure 33. Gene expression results of the *OeSMT2* (Error bars represent standard error and asterisks represent statistically significant differences at $P < 0.05$ based on Tukey's test).

When the *OeSMT2.1* gene expression results were assessed in general, a similar expression pattern was observed with *OeSMT2* except for a few minor differences. Especially in the period starting from August 15 to November 1, elevated levels were noticed in the expression of this gene in the Gökçeada cultivar compared to other cultivars. In a study that involved our Lab team, the final PS content of these four cultivars was examined simultaneously with *OeSMT* gene expression, and a non-negligible increase was observed in the total PS content in four cultivars after September 15. Among the four olive cultivars, remarkably higher expression of *OeSMT2* was observed in Gökçeada, and these results were actually consistent with the highest concentration of PS detected in the oil of the Gökçeada cultivar (Figure 2 Suppl.). In addition, the reduction in *OeSMT2* gene expression seen on August 1 was also observed in the *OeSMT2.1* (Figure 34).

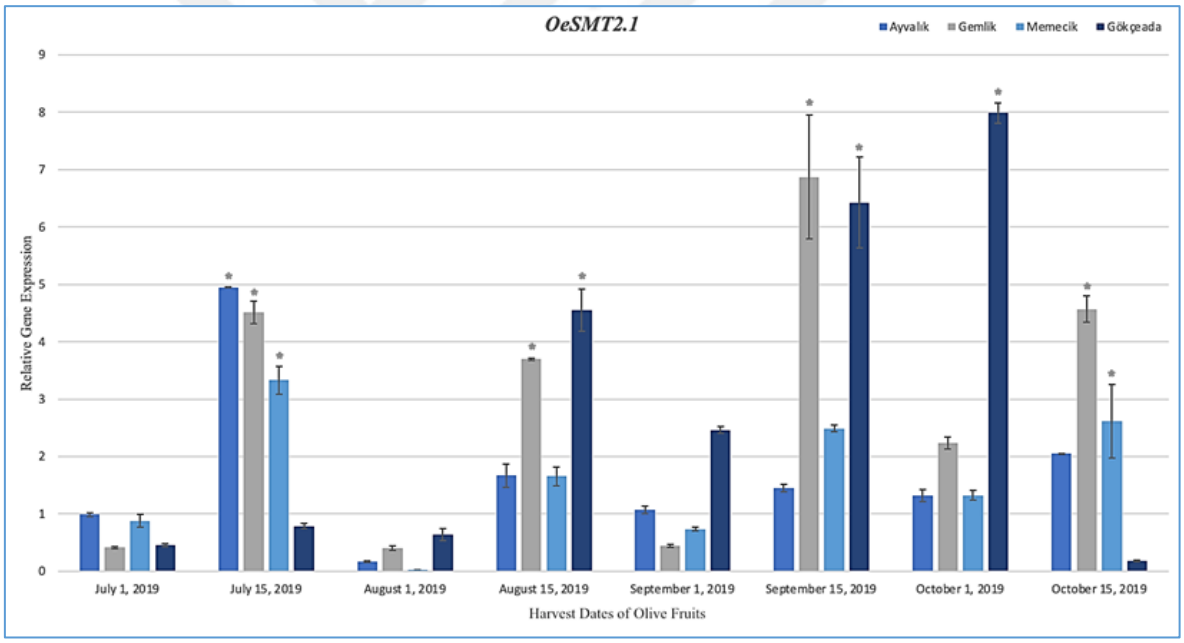

Figure 34. Gene expression results of the *OeSMT2.1* (Error bars represent standard error and asterisks represent statistically significant differences at P <0.05 based on Tukey's test).

CHAPTER 5

CONCLUSION

The objective of this study is to identify the *SMT* genes proven to play roles in the key points of PS synthase in the olive genome and to examine the expression levels of these genes during olive fruit ripening. With this aim, olive fruits of Ayvalık, Gemlik, Memecik, and Gökçeada cultivars, which are widely grown in Türkiye, were obtained through 8 consecutive fruit ripening periods and molecular factors affecting the expression of *OeSMT* genes were revealed. Moreover the sequences of olive *SMT* genes (*OeSMT1* and *OeSMT2*) were determined for the first time.

In higher plants, the synthesis of PSs starts with mevalonate synthesis from acetyl CoA and includes sequential numerous enzymatic reactions. Along through this biosynthetic pathway, some enzymes are considerably important with their critical activities such as sterol methyl transferases which sustain the carbon flux (Holmberg et al., 2002). *SMT 1* provides the methylation of cycloartenol and its rate-limiting action affects the final sterol concentration. The second methylation is provided by the other member of sterol transferases, *SMT2*, which is crucial for the balance in the final concentration between 24-methyl and 24-ethyl sterol (Schaeffer et al., 2001). Here in the present study, the *SMT* genes were identified in the *Olea europaea* var. *Sylvestris* genome with bioinformatic studies. Obtained results demonstrate that two separate *SMT* genes are found in the Sylvestris genome, unlike the model organism *Arabidopsis*, which contains three different *SMT* genes (*SMT1, SMT2,* and *SMT3*) responsible for coding sterol methyl transferases. The phylogenetic tree plotted with reference *SMT* sequences of *A. thaliana* and *S. lycopersicum* was shown that *OeSMTs* are located in two separate branches. The cloning of *OeSMT* genes was completed successfully and the sequence of these genes was determined for the first time in the *Olea europaea* L. genome. The identity of *OeSMTs* was searched by BLASTn analysis with the other plant species. According to obtained data, it was observed that *OeSMT1* has the highest relativeness with *Erythranthe guttatus* species, while *OeSMT2.1* and *OeSMT2.2* are most alike with *Sesamum indicum* species. A phylogenetic tree was plotted with sequences of the other plant species and the separation of *OeSMT1* and *OeSMT2* genes into two different branches in this tree was observed as expected.

At the final stage of this study the gene-specific primers were designed and the expression of *OeSMT*s was investigated in four olive cultivars along the fruit ripening. In the early phases of fruit ripening, an active expression of *OeSMT1* was detected with only slight variations between 4 olive cultivars whereas a constantly active expression in *OeSMT2* was observed during all stages of fruit ripening.

Olive is a widely grown harvest plant in Türkiye and is of great importance with its rich nutritional content in its oil. In this respect, it is important to obtain olive varieties with high PS content and to determine the optimal harvest date for olives during the periods when the PS content is highest. Gene expression and sequencing data of *OeSMT*s obtained with this research light the way molecular breeding studies for the selection of cultivars with high PS content in olive species.

REFERENCES

Benveniste, P. (2004). Biosynthesis and accumulation of sterols. *Annual Review of Plant Biology*, *55*, 429–457. https://doi.org/10.1146/annurev.arplant.55.031903.141616

Bouic, P. J. D., Etsebeth, S., Liebenberg, R. W., Albrecht, C. F., & Pegel, K. (1997). *BETA-SITOSTEROL A N D BETA-SITOSTEROL GLUCOSIDE STIMULATE H U M A N P E R I P H E R A L BLOOD LYMPHOCYTE PROLIFERATION : IMPLICATIONS FOR T H E I R USE AS A N I M M U N O M O D U L A T O R Y VITAMIN COMBINATION *. *18*(12).

Bouvier-Navé, P., Husselstein, T., & Benveniste, P. (1998). Two families of sterol methyltransferases are involved in the first and the second methylation steps of plant sterol biosynthesis. *European Journal of Biochemistry*, *256*(1), 88–96. https://doi.org/10.1046/j.1432-1327.1998.2560088.x

Bouvier-Navé, P., Husselstein, T., Desprez, T., & Benveniste, P. (1997). Identification of cDNAs encoding sterol methyl-transferases involved in the second methylation step of plant sterol biosynthesis. *European Journal of Biochemistry*, *246*(2), 518–529. https://doi.org/10.1111/j.1432-1033.1997.t01-1-00518.x

Bracci, T., Busconi, M., Fogher, C., & Sebastiani, L. (2011). Molecular studies in olive (Olea europaea L.): Overview on DNA markers applications and recent advances in genome analysis. *Plant Cell Reports*, *30*(4), 449–462. https://doi.org/10.1007/s00299-010-0991-9

Brown, R. E. (1998). Sphingolipid organization in biomembranes: What physical studies of model membranes reveal. *Journal of Cell Science*, *111*(1), 1–9. https://doi.org/10.1242/jcs.111.1.1

Carland, F., Fujioka, S., & Nelson, T. (2010). The sterol methyltransferases SMT1, SMT2, and SMT3 influence arabidopsis development through nonbrassinosteroid products. *Plant Physiology*, *153*(2), 741–756. https://doi.org/10.1104/pp.109.152587

Carland, F. M., Fujioka, S., Takatsuto, S., Yoshida, S., & Nelson, T. (2002). The identification of CVP1 reveals a role for sterols in vascular patterning. *Plant Cell*, *14*(9), 2045–2058. https://doi.org/10.1105/tpc.003939

Choe, S., Dilkes, B. P., Gregory, B. D., Ross, A. S., Yuan, H., Noguchi, T., Fujioka, S., Takatsuto, S., Tanaka, A., Yoshida, S., Tax, F. E., & Feldmann, K. A. (1999). The Arabidopsis dwarf1 mutant is defective in the conversion of 24-methylenecholesterol to campesterol in brassinosteroid biosynthesis. *Plant Physiology*, *119*(3), 897–907. https://doi.org/10.1104/pp.119.3.897

Diener, A. C., Li, H., Zhou, W. X., Whoriskey, W. J., Nes, W. D., & Fink, G. R. (2000). STEROL METHYLTRANSFERASE 1 controls the level of cholesterol in plants. *Plant Cell*, *12*(6), 853–870. https://doi.org/10.1105/tpc.12.6.853

Dorak, M. T. (2007). *Real-time PCR*. Taylor & Francis.

Dufourc, E. J. (2008). The role of phytosterols in plant adaptation to temperature. *Plant Signaling and Behavior*, *3*(2), 133–134. https://doi.org/10.4161/psb.3.2.5051

Efe, R., Soykan, A., Curebal, I., & Sonimez, S. (2013). *Olive and Olive Oil in Edremit Region*. https://www.academia.edu/4050585/Olive_and_Olive_Oil_Ecology_of_Olive_in_Turkey

Feng, S., Wang, L., Shao, P., Sun, P., & Yang, C. S. (2021). A review on chemical and physical modifications of phytosterols and their influence on bioavailability and safety. *Critical Reviews in Food Science and Nutrition*, *62*(20), 5638–5657. https://doi.org/10.1080/10408398.2021.1888692

Fernández-Cuesta, A., León, L., Velasco, L., & De la Rosa, R. (2013). Changes in squalene and sterols associated with olive maturation. *Food Research International*, *54*(2), 1885–1889. https://doi.org/10.1016/j.foodres.2013.07.049

Grebenok, R. J., Galbraith, D. W., & Della Penna, D. (1997). Characterization of Zea mays endosperm C-24 sterol methyltransferase: One of two types of sterol methyltransferase in higher plants. *Plant Molecular Biology*, *34*(6), 891–896. https://doi.org/10.1023/A:1005818210641

Gül, M. K., & Şeker, M. (2006). Comparative analysis of phytosterol components from rapeseed (Brassica napus L.) and olive (Olea europaea L.) varieties. *European Journal of Lipid Science and Technology*, *108*(9), 759–765. https://doi.org/10.1002/ejlt.200600085

Hartmann, M. A. (1998). Plant sterols and the membrane environment. *Trends in Plant Science*, *3*(5), 170–175. https://doi.org/10.1016/S1360-1385(98)01233-3

Hatzopoulos, P., Banilas, G., Giannoulia, K., Gazis, F., Nikoloudakis, N., Milioni, D., & Haralampidis, K. (2002). Breeding, molecular markers and molecular biology of the olive tree. *European Journal of Lipid Science and Technology*, *104*(9–10), 574–586. https://doi.org/10.1002/1438-9312(200210)104:9/10<574::AID-EJLT574>3.0.CO;2-1

Holmberg, N., Harker, M., Gibbard, C. L., Wallace, A. D., Clayton, J. C., Rawlins, S., Hellyer, A., & Safford, R. (2002). Sterol C-24 methyltransferase type 1 controls the flux of carbon into sterol biosynthesis in tobacco seed. *Plant Physiology*, *130*(1), 303–311. https://doi.org/10.1104/pp.004226

Hürkan, K., Sezer, F., Özbilen, A., & Taşkın, K. M. (2018). Identification of reference genes for real-time quantitative polymerase chain reaction based gene expression studies on various Olive (Olea europaea L.) tissues. *Journal of Horticultural Science and Biotechnology*, *93*(6), 644–651. https://doi.org/10.1080/14620316.2018.1427005

Inês, C., Corbacho, J., Paredes, M. A., Labrador, J., Cordeiro, A. M., & Gomez-Jimenez, M. C. (2019). Regulation of sterol content and biosynthetic gene expression during flower opening and early fruit development in olive. *Physiologia Plantarum*, *167*(4), 526–539. https://doi.org/10.1111/ppl.12969

Kyçyk, O., Aguilera, M. P., Gaforio, J. J., Jiménez, A., & Beltrán, G. (2016). Sterol composition of virgin olive oil of forty-three olive cultivars from the World Collection Olive Germplasm Bank of Cordoba. *Journal of the Science of Food and Agriculture*, *96*(12), 4143–4150. https://doi.org/10.1002/jsfa.7616

Li, J., Nagpal, P., Vitart, V., Mcmorris, T. C., & Chorys, J. (1996). *3). -5. April*.

Miras-Moreno, B., Sabater-Jara, A. B., Pedreno, M. A., & Almagro, L. (2016). Bioactivity of Phytosterols and Their Production in Plant in Vitro Cultures. *Journal of Agricultural and Food Chemistry*, *64*(38), 7049–7058. https://doi.org/10.1021/acs.jafc.6b02345

Mohammadi, M., Jafari, S. M., Hamishehkar, H., & Ghanbarzadeh, B. (2020). Phytosterols as the core or stabilizing agent in different nanocarriers. *Trends in Food Science and Technology*, *101*(April), 73–88. https://doi.org/10.1016/j.tifs.2020.05.004

Mongrand, S., Morel, J., Laroche, J., Claverol, S., Carde, J. P., Hartmann, M. A., Bonneu, M., Simon-Plas, F., Lessire, R., & Bessoule, J. J. (2004). Lipid rafts in higher plant cells: Purification and characterization of triton X-100-insoluble microdomains from tobacco plasma membrane. *Journal of Biological Chemistry*, *279*(35), 36277–36286. https://doi.org/10.1074/jbc.M403440200

Moreau, R. A., Whitaker, B. D., & Hicks, K. B. (2002). Phytosterols, phytostanols, and their conjugates in foods: Structural diversity, quantitative analysis, and health-promoting uses. *Progress in Lipid Research*, *41*(6), 457–500. https://doi.org/10.1016/S0163-7827(02)00006-1

Nakamoto, M., Schmit, A. C., Heintz, D., Schaller, H., & Ohta, D. (2015). Diversification of sterol methyltransferase enzymes in plants and a role for β-sitosterol in oriented cell plate formation and polarized growth. *Plant Journal*, *84*(5), 860–874. https://doi.org/10.1111/tpj.13043

Nattagh-eshtivani, E. (2022). *Biological and pharmacological effects and nutritional impact of phytosterols : A comprehensive review*. *September 2021*, 299–322. https://doi.org/10.1002/ptr.7312

Navas-López, J. F., Cano, J., de la Rosa, R., Velasco, L., & León, L. (2020). Genotype by environment interaction for oil quality components in olive tree. *European Journal of Agronomy*, *119*(June), 126115. https://doi.org/10.1016/j.eja.2020.126115

Neelakandan, A. K., Song, Z., Wang, J., Richards, M. H., Wu, X., Valliyodan, B., Nguyen, H. T., & Nes, W. D. (2009). Cloning, functional expression and phylogenetic analysis of plant sterol 24C-methyltransferases involved in sitosterol biosynthesis. *Phytochemistry*, *70*(17–18), 1982–1998. https://doi.org/10.1016/j.phytochem.2009.09.003

Nes, W. D. (2000). Sterol methyl transferase: Enzymology and inhibition. *Biochimica et Biophysica Acta - Molecular and Cell Biology of Lipids*, *1529*(1–3), 63–88. https://doi.org/10.1016/S1388-1981(00)00138-4

Nes, W. D. (2011). Biosynthesis of cholesterol and other sterols. *Chemical Reviews*, *111*(10), 6423–6451. https://doi.org/10.1021/cr200021m

Nes, W. D., Song, Z., Dennis, A. L., Zhou, W., Nam, J., & Miller, M. B. (2003).

Biosynthesis of phytosterols: Kinetic mechanism for the enzymatic C-methylation of sterols. *Journal of Biological Chemistry*, *278*(36), 34505–34516. https://doi.org/10.1074/jbc.M303359200

Orem, A., Alasalvar, C., Vanizor Kural, B., Yaman, S., Orem, C., Karadag, A., Pelvan, E., & Zawistowski, J. (2017). Cardio-protective effects of phytosterol-enriched functional black tea in mild hypercholesterolemia subjects. *Journal of Functional Foods*, *31*, 311–319. https://doi.org/10.1016/j.jff.2017.01.048

Ozkan, A., Aboul-Enein, H. Y., Kulak, M., & Bindak, R. (2017). Comparative study on fatty acid composition of olive (Olea europaea L.), with emphasis on phytosterol contents. *Biomedical Chromatography*, *31*(8), 1–7. https://doi.org/10.1002/bmc.3933

Pfaffl, M. W. (2001). A new mathematical model for relative quantification in real-time RT–PCR. *Nucleic Acids Research*, *29*(9), e45–e45. https://doi.org/10.1093/nar/29.9.e45

Piironen, V., Lindsay, D. G., Miettinen, T. A., Toivo, J., & Lampi, A. M. (2000). Plant sterols: Biosynthesis, biological function and their importance to human nutrition. *Journal of the Science of Food and Agriculture*, *80*(7), 939–966. https://doi.org/10.1002/(SICI)1097-0010(20000515)80:7<939::AID-JSFA644>3.0.CO;2-C

Quílez, J., García-Lorda, P., & Salas-Salvadó, J. (2003). Potential uses and benefits of phytosterols in diet: Present situation and future directions. *Clinical Nutrition*, *22*(4), 343–351. https://doi.org/10.1016/S0261-5614(03)00060-8

Ramos, A., Rapoport, H. F., Cabello, D., & Rallo, L. (2018). Chilling accumulation, dormancy release temperature, and the role of leaves in olive reproductive budburst: Evaluation using shoot explants. *Scientia Horticulturae*, *231*(November 2017), 241–252. https://doi.org/10.1016/j.scienta.2017.11.003

Schaeffer, A., Bronner, R., Benveniste, P., & Schaller, H. (2001). The ratio of campesterol to sitosterol that modulates growth in Arabidopsis is controlled by STEROL METHYLTRANSFERASE 2;i. *Plant Journal*, *25*(6), 605–615. https://doi.org/10.1046/j.1365-313X.2001.00994.x

Schaller, H. (2003). The role of sterols in plant growth and development. *Progress in Lipid*

Research, *42*(3), 163–175. https://doi.org/10.1016/S0163-7827(02)00047-4

Schaller, H., Bouvier-Navé, P., & Benveniste, P. (1998). Overexpression of an arabidopsis cDNA encoding a sterol-C241-methyltransferase in tobacco modifies the ratio of 24-methyl cholesterol to sitosterol and is associated with growth reduction. *Plant Physiology*, *118*(2), 461–469. https://doi.org/10.1104/pp.118.2.461

Schrick, K., Fujioka, S., Takatsuto, S., Stierhof, Y. D., Stransky, H., Yoshida, S., & Jürgens, G. (2004). A link between sterol biosynthesis, the cell wall, and cellulose in Arabidopsis. *Plant Journal*, *38*(2), 227–243. https://doi.org/10.1111/j.1365-313X.2004.02039.x

Shenouda, N., Sakla, M., Newton, L., Besch-Williford, C., Greenberg, N., MacDonald, R., & Lubahn, D. (2007). Phytosterol Pygeum africanum regulates prostate cancer in vitro and in vivo. *Endocrine*, *31*(1), 72–81. https://doi.org/10.1007/s12020-007-0014-y

Sivakumar, G., Bati, C. B., Perri, E., & Uccella, N. (2006). Gas chromatography screening of bioactive phytosterols from mono-cultivar olive oils. *Food Chemistry*, *95*(3), 525–528. https://doi.org/10.1016/j.foodchem.2005.04.003

Valitova, J. N., Sulkarnayeva, A. G., & Minibayeva, F. V. (2016). Plant sterols: Diversity, biosynthesis, and physiological functions. *Biochemistry (Moscow)*, *81*(8), 819–834. https://doi.org/10.1134/S0006297916080046

Willemsen, V., Friml, J., Grebe, M., Van Den Toorn, A., Palme, K., & Scheres, B. (2003). Cell polarity and PIN protein positioning in Arabidopsis require STEROL METHYLTRANSFERASE1 function. *Plant Cell*, *15*(3), 612–625. https://doi.org/10.1105/tpc.008433

Yang, R., Xue, L., Zhang, L., Wang, X., Qi, X., Jiang, J., Yu, L., Wang, X., Zhang, W., Zhang, Q., & Li, P. (2019). Phytosterol contents of edible oils and their contributions to estimated phytosterol intake in the Chinese diet. *Foods*, *8*(8). https://doi.org/10.3390/foods8080334

APPENDIX

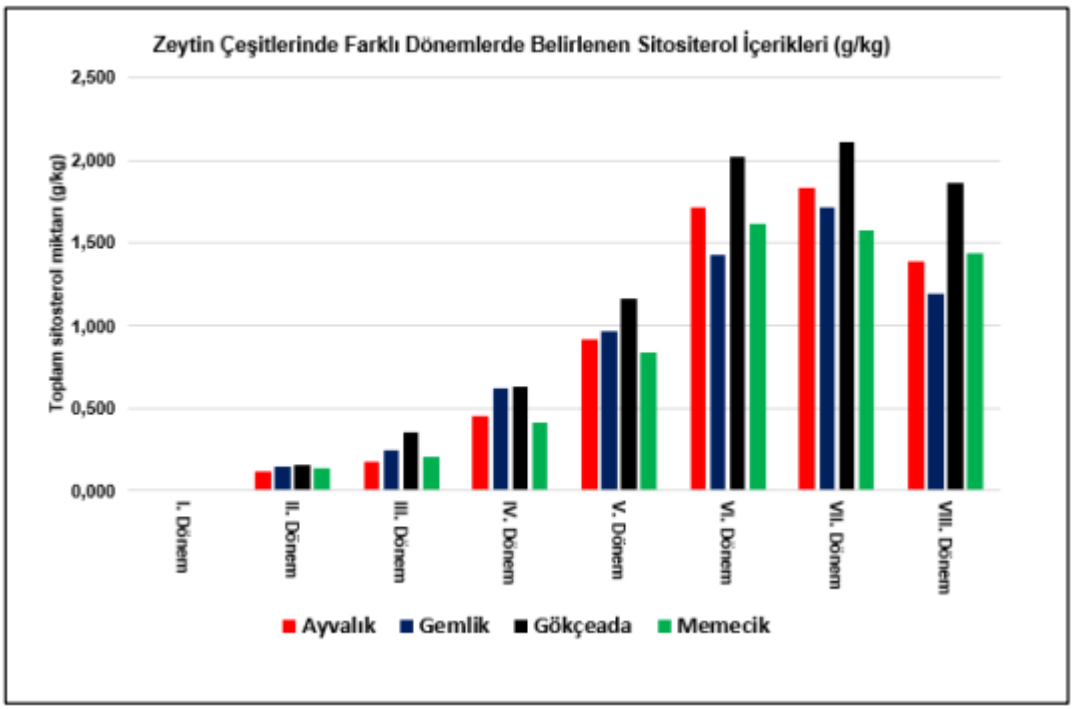

Figure 1. Variation of *β*-sitosterol contents determined in different periods in olive cultivars (Unpublished data from project 118O405 funded by TÜBİTAK).

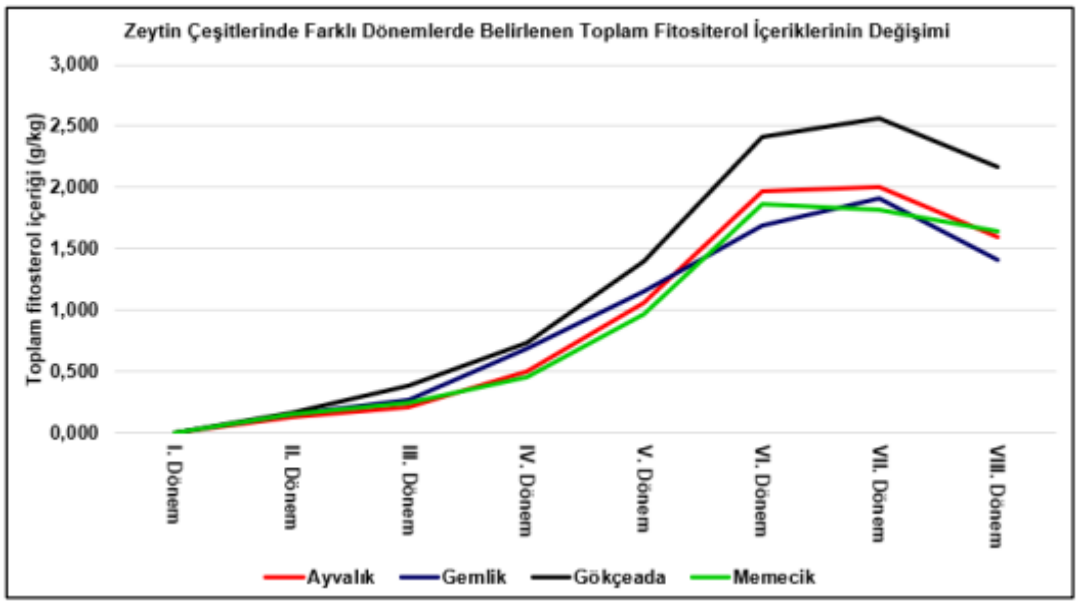

Figure 2. The change of total phytosterol contents throughout 8 different ripening periods in 4 olive cultivars (Unpublished data from project 118O405 funded by TÜBİTAK).

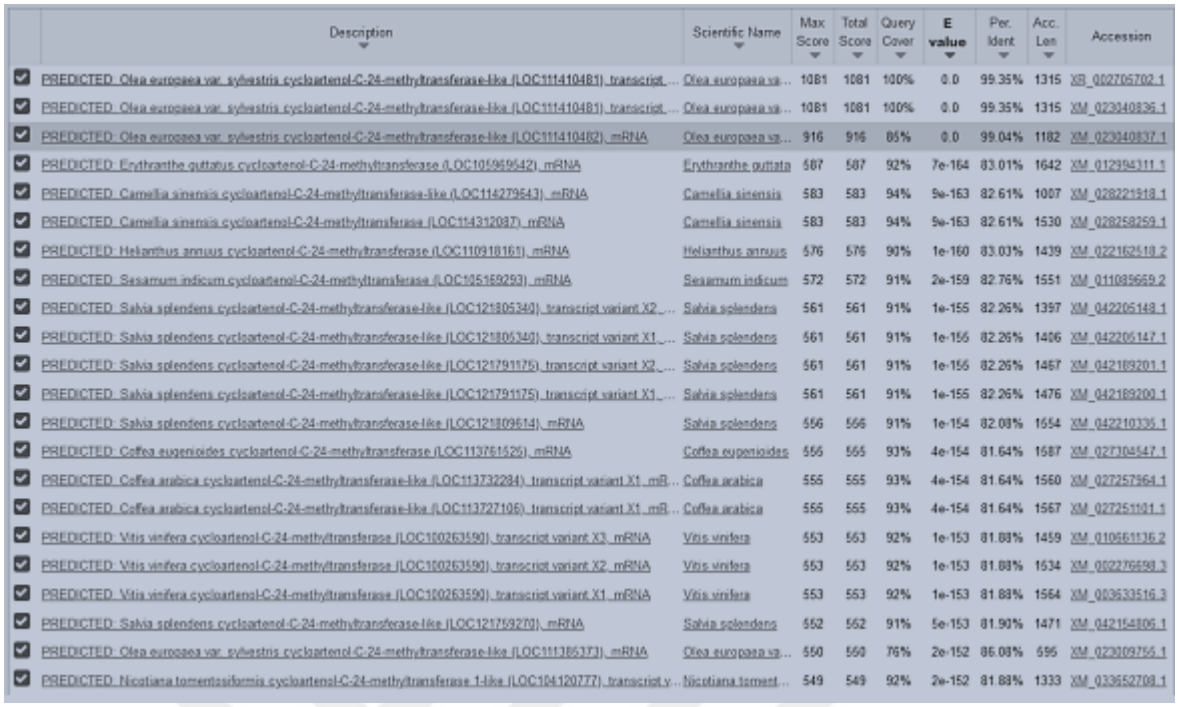

Description	Scientific Name	Max Score	Total Score	Query Cover	E value	Per. Ident	Acc. Len	Accession
PREDICTED: Olea europaea var. sylvestris cycloartenol-C-24-methyltransferase-like (LOC111410481), transcript ...	Olea europaea va...	1081	1081	100%	0.0	99.35%	1315	XR_002705702.1
PREDICTED: Olea europaea var. sylvestris cycloartenol-C-24-methyltransferase-like (LOC111410481), transcript ...	Olea europaea va...	1081	1081	100%	0.0	99.35%	1315	XM_023040836.1
PREDICTED: Olea europaea var. sylvestris cycloartenol-C-24-methyltransferase-like (LOC111410482), mRNA	Olea europaea va...	916	916	85%	0.0	99.04%	1182	XM_023040837.1
PREDICTED: Erythranthe guttatus cycloartenol-C-24-methyltransferase (LOC105969542), mRNA	Erythranthe guttata	587	587	92%	7e-164	83.01%	1642	XM_012994311.1
PREDICTED: Camellia sinensis cycloartenol-C-24-methyltransferase-like (LOC114279643), mRNA	Camellia sinensis	583	583	94%	9e-163	82.61%	1007	XM_028221918.1
PREDICTED: Camellia sinensis cycloartenol-C-24-methyltransferase (LOC114312087), mRNA	Camellia sinensis	583	583	94%	9e-163	82.61%	1530	XM_028258259.1
PREDICTED: Helianthus annuus cycloartenol-C-24-methyltransferase (LOC110918161), mRNA	Helianthus annuus	576	576	90%	1e-160	83.03%	1439	XM_022162518.2
PREDICTED: Sesamum indicum cycloartenol-C-24-methyltransferase (LOC105159293), mRNA	Sesamum indicum	572	572	91%	2e-159	82.76%	1551	XM_011089669.2
PREDICTED: Salvia splendens cycloartenol-C-24-methyltransferase-like (LOC121805340), transcript variant X2 ...	Salvia splendens	561	561	91%	1e-155	82.26%	1397	XM_042206148.1
PREDICTED: Salvia splendens cycloartenol-C-24-methyltransferase-like (LOC121805340), transcript variant X1 ...	Salvia splendens	561	561	91%	1e-155	82.26%	1406	XM_042206147.1
PREDICTED: Salvia splendens cycloartenol-C-24-methyltransferase-like (LOC121791175), transcript variant X2 ...	Salvia splendens	561	561	91%	1e-155	82.26%	1467	XM_042189201.1
PREDICTED: Salvia splendens cycloartenol-C-24-methyltransferase-like (LOC121791175), transcript variant X1 ...	Salvia splendens	561	561	91%	1e-155	82.26%	1476	XM_042189200.1
PREDICTED: Salvia splendens cycloartenol-C-24-methyltransferase-like (LOC121809514), mRNA	Salvia splendens	556	556	91%	1e-154	82.08%	1554	XM_042210335.1
PREDICTED: Coffea eugenioides cycloartenol-C-24-methyltransferase (LOC113761525), mRNA	Coffea eugenioides	555	555	93%	4e-154	81.64%	1587	XM_027104547.1
PREDICTED: Coffea arabica cycloartenol-C-24-methyltransferase-like (LOC113732284), transcript variant X1, mR...	Coffea arabica	555	555	93%	4e-154	81.64%	1560	XM_027257364.1
PREDICTED: Coffea arabica cycloartenol-C-24-methyltransferase-like (LOC113727106), transcript variant X1, mR...	Coffea arabica	555	555	93%	4e-154	81.64%	1567	XM_027251101.1
PREDICTED: Vitis vinifera cycloartenol-C-24-methyltransferase (LOC100263590), transcript variant X3, mRNA	Vitis vinifera	553	553	92%	1e-153	81.88%	1459	XM_010661136.2
PREDICTED: Vitis vinifera cycloartenol-C-24-methyltransferase (LOC100263590), transcript variant X2, mRNA	Vitis vinifera	553	553	92%	1e-153	81.88%	1534	XM_002276598.3
PREDICTED: Vitis vinifera cycloartenol-C-24-methyltransferase (LOC100263590), transcript variant X1, mRNA	Vitis vinifera	553	553	92%	1e-153	81.88%	1564	XM_003633516.3
PREDICTED: Salvia splendens cycloartenol-C-24-methyltransferase-like (LOC121759270), mRNA	Salvia splendens	552	552	91%	5e-153	81.90%	1471	XM_042154806.1
PREDICTED: Olea europaea var. sylvestris cycloartenol-C-24-methyltransferase-like (LOC111385173), mRNA	Olea europaea va...	550	550	76%	2e-152	86.08%	595	XM_023009755.1
PREDICTED: Nicotiana tomentosiformis cycloartenol-C-24-methyltransferase 1-like (LOC104120777), transcript v...	Nicotiana toment...	549	549	92%	2e-152	81.88%	1333	XM_033652708.1

Figure 3. BLASTn result of *OeSMT1*

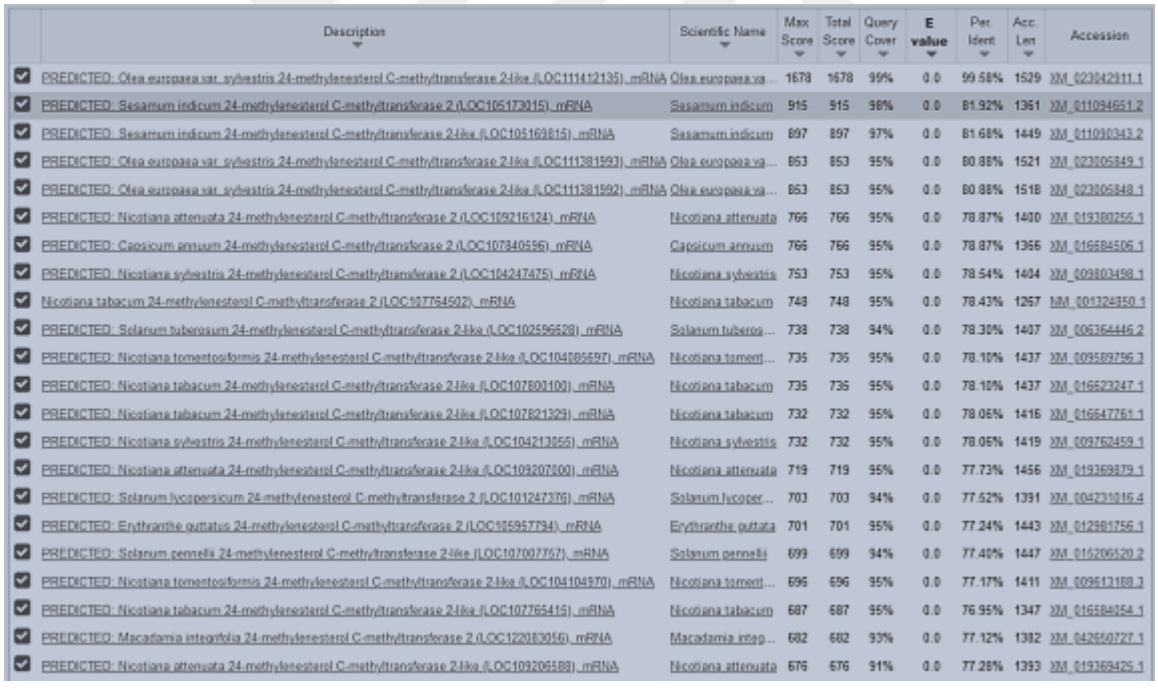

Description	Scientific Name	Max Score	Total Score	Query Cover	E value	Per. Ident	Acc. Len	Accession
PREDICTED: Olea europaea var. sylvestris 24-methylenesterol C-methyltransferase 2-like (LOC111412135), mRNA	Olea europaea va...	1678	1678	99%	0.0	99.58%	1529	XM_023042911.1
PREDICTED: Sesamum indicum 24-methylenesterol C-methyltransferase 2 (LOC105173015), mRNA	Sesamum indicum	915	915	98%	0.0	81.92%	1361	XM_011094651.2
PREDICTED: Sesamum indicum 24-methylenesterol C-methyltransferase 2-like (LOC105169815), mRNA	Sesamum indicum	897	897	97%	0.0	81.68%	1449	XM_011090343.2
PREDICTED: Olea europaea var. sylvestris 24-methylenesterol C-methyltransferase 2-like (LOC111381593), mRNA	Olea europaea va...	853	853	95%	0.0	80.88%	1521	XM_023005849.1
PREDICTED: Olea europaea var. sylvestris 24-methylenesterol C-methyltransferase 2-like (LOC111381592), mRNA	Olea europaea va...	853	853	95%	0.0	80.88%	1518	XM_023005848.1
PREDICTED: Nicotiana attenuata 24-methylenesterol C-methyltransferase 2 (LOC109216124), mRNA	Nicotiana attenuata	766	766	95%	0.0	78.87%	1400	XM_019380255.1
PREDICTED: Capsicum annuum 24-methylenesterol C-methyltransferase 2 (LOC107840556), mRNA	Capsicum annuum	766	766	95%	0.0	78.87%	1366	XM_016584506.1
PREDICTED: Nicotiana sylvestris 24-methylenesterol C-methyltransferase 2 (LOC104247475), mRNA	Nicotiana sylvestris	753	753	95%	0.0	78.54%	1404	XM_009803498.1
Nicotiana tabacum 24-methylenesterol C-methyltransferase 2 (LOC107754502), mRNA	Nicotiana tabacum	748	748	95%	0.0	78.43%	1267	NM_001324350.1
PREDICTED: Solanum tuberosum 24-methylenesterol C-methyltransferase 2-like (LOC102596528), mRNA	Solanum tubero...	738	738	94%	0.0	78.30%	1407	XM_006364446.2
PREDICTED: Nicotiana tomentosiformis 24-methylenesterol C-methyltransferase 2-like (LOC104086597), mRNA	Nicotiana toment...	735	735	95%	0.0	78.10%	1437	XM_009589796.3
PREDICTED: Nicotiana tabacum 24-methylenesterol C-methyltransferase 2-like (LOC107800100), mRNA	Nicotiana tabacum	735	735	95%	0.0	78.10%	1437	XM_016523247.1
PREDICTED: Nicotiana tabacum 24-methylenesterol C-methyltransferase 2-like (LOC107821329), mRNA	Nicotiana tabacum	732	732	95%	0.0	78.06%	1416	XM_016647761.1
PREDICTED: Nicotiana sylvestris 24-methylenesterol C-methyltransferase 2-like (LOC104213555), mRNA	Nicotiana sylvestris	732	732	95%	0.0	78.06%	1419	XM_009762459.1
PREDICTED: Nicotiana attenuata 24-methylenesterol C-methyltransferase 2-like (LOC109207500), mRNA	Nicotiana attenuata	719	719	95%	0.0	77.73%	1456	XM_019369879.1
PREDICTED: Solanum lycopersicum 24-methylenesterol C-methyltransferase 2 (LOC101247376), mRNA	Solanum lycoper...	703	703	94%	0.0	77.52%	1391	XM_004231016.4
PREDICTED: Erythranthe guttatus 24-methylenesterol C-methyltransferase 2 (LOC105957794), mRNA	Erythranthe guttata	701	701	95%	0.0	77.24%	1443	XM_012981756.1
PREDICTED: Solanum pennellii 24-methylenesterol C-methyltransferase 2-like (LOC107007767), mRNA	Solanum pennellii	699	699	94%	0.0	77.46%	1447	XM_015206520.2
PREDICTED: Nicotiana tomentosiformis 24-methylenesterol C-methyltransferase 2-like (LOC104104970), mRNA	Nicotiana toment...	696	696	95%	0.0	77.17%	1411	XM_009613188.3
PREDICTED: Nicotiana tabacum 24-methylenesterol C-methyltransferase 2-like (LOC107765415), mRNA	Nicotiana tabacum	687	687	95%	0.0	76.95%	1347	XM_016589054.1
PREDICTED: Macadamia integrifolia 24-methylenesterol C-methyltransferase 2 (LOC122083056), mRNA	Macadamia integ...	682	682	93%	0.0	77.12%	1382	XM_042550727.1
PREDICTED: Nicotiana attenuata 24-methylenesterol C-methyltransferase 2-like (LOC109206588), mRNA	Nicotiana attenuata	676	676	91%	0.0	77.28%	1393	XM_019369425.1

Figure 4. BLASTn result of *OeSMT2.1*

Description	Scientific Name	Max Score	Total Score	Query Cover	E value	Per. Ident	Acc. Len	Accession
PREDICTED: Olea europaea var. sylvestris 24-methylenesterol C-methyltransferase 2-like (LOC111381993), mRNA	Olea europaea va...	2244	2244	99%	0.0	99.37%	1521	XM_023005849.1
PREDICTED: Olea europaea var. sylvestris 24-methylenesterol C-methyltransferase 2-like (LOC111381992), mRNA	Olea europaea va...	2244	2244	99%	0.0	99.37%	1518	XM_023005848.1
PREDICTED: Olea europaea var. sylvestris 24-methylenesterol C-methyltransferase 2-like (LOC111412135), mRNA	Olea europaea va...	977	977	85%	0.0	80.16%	1529	XM_023042911.1
PREDICTED: Sesamum indicum 24-methylenesterol C-methyltransferase 2-like (LOC105165815), mRNA	Sesamum indicum	963	963	85%	0.0	79.80%	1449	XM_011080343.2
PREDICTED: Sesamum indicum 24-methylenesterol C-methyltransferase 2 (LOC105173015), mRNA	Sesamum indicum	940	940	84%	0.0	79.61%	1361	XM_011094651.2
PREDICTED: Ipomoea triloba 24-methylenesterol C-methyltransferase 2-like (LOC116996133), mRNA	Ipomoea triloba	824	824	85%	0.0	76.92%	1525	XM_031235276.1
PREDICTED: Nicotiana tomentosiformis 24-methylenesterol C-methyltransferase 2-like (LOC104104970), mRNA	Nicotiana toment...	819	819	85%	0.0	76.98%	1411	XM_009613188.3
PREDICTED: Nicotiana tomentosiformis 24-methylenesterol C-methyltransferase 2-like (LOC104085697), mRNA	Nicotiana toment...	817	817	83%	0.0	77.09%	1437	XM_009589796.3
PREDICTED: Nicotiana attenuata 24-methylenesterol C-methyltransferase 2-like (LOC109207000), mRNA	Nicotiana attenuata	817	817	86%	0.0	76.63%	1456	XM_019369879.1
PREDICTED: Nicotiana tabacum 24-methylenesterol C-methyltransferase 2-like (LOC107801000), mRNA	Nicotiana tabacum	817	817	83%	0.0	77.09%	1437	XM_016523247.1
PREDICTED: Nicotiana tabacum 24-methylenesterol C-methyltransferase 2-like (LOC107765415), mRNA	Nicotiana tabacum	814	814	85%	0.0	76.89%	1347	XM_016584064.1
PREDICTED: Coffea eugenioides 24-methylenesterol C-methyltransferase 2-like (LOC113736564), mRNA	Coffea eugenioides	813	813	83%	0.0	77.06%	1524	XM_027329868.1
PREDICTED: Coffea arabica 24-methylenesterol C-methyltransferase 2-like (LOC113710393), mRNA	Coffea arabica	813	813	83%	0.0	77.06%	1530	XM_027233364.1
Nicotiana tabacum 24-methylenesterol C-methyltransferase 2 (LOC107764502), mRNA	Nicotiana tabacum	809	809	83%	0.0	76.96%	1267	NM_001324650.1
PREDICTED: Nicotiana sylvestris 24-methylenesterol C-methyltransferase 2 (LOC104247475), mRNA	Nicotiana sylvestris	809	809	83%	0.0	76.96%	1404	XM_009803498.1
PREDICTED: Nicotiana attenuata 24-methylenesterol C-methyltransferase 2 (LOC109216124), mRNA	Nicotiana attenuata	804	804	83%	0.0	76.87%	1400	XM_019392255.1
PREDICTED: Coffea arabica 24-methylenesterol C-methyltransferase 2-like (LOC113708954), misc_RNA	Coffea arabica	797	797	83%	0.0	76.97%	1531	XR_003452543.1
PREDICTED: Ipomoea nil 24-methylenesterol C-methyltransferase 2 (LOC109162135), mRNA	Ipomoea nil	795	795	84%	0.0	76.48%	1480	XM_019310847.1
PREDICTED: Nicotiana tabacum 24-methylenesterol C-methyltransferase 2-like (LOC107821329), mRNA	Nicotiana tabacum	780	780	86%	0.0	76.02%	1416	XM_016647761.1
PREDICTED: Erythranthe guttatus 24-methylenesterol C-methyltransferase 2 (LOC105957794), mRNA	Erythranthe guttata	780	780	84%	0.0	76.25%	1443	XM_012981756.1
PREDICTED: Nicotiana sylvestris 24-methylenesterol C-methyltransferase 2-like (LOC104213055), mRNA	Nicotiana sylvestris	780	780	86%	0.0	76.02%	1419	XM_009762459.1
PREDICTED: Solanum tuberosum 24-methylenesterol C-methyltransferase 2-like (LOC102596628), mRNA	Solanum tuberos...	766	766	83%	0.0	76.10%	1407	XM_006364446.2

Figure 5. BLASTn result of *OeSMT2.2*